ISSN 1070-3632, Russian Journal of General Chemistry, 2021, Vol. 91, Suppl. 1, pp. S60–S83. © Pleiades Publishing, Ltd., 2021.
Russian Text © The Author(s), 2021, published in Rossiiskii Khimicheskii Zhurnal, 2021, Vol. 65, No. 4, pp. 12–35.

The Influence of the Structure of Pectin Substances of Flax Fodder Supplements on Absorption Binding of Azaheterocyclic Mycotoxins

S. A. Koksharov[a],*, S. V. Aleeva[a],, and O. V. Lepilova[a],*****

[a] *G.A. Krestov Institute of Solution Chemistry of the Russian Academy of Sciences, Ivanovo, 153045 Russia*
**e-mail: ksa@isc-ras.ru; **e-mail: sva@isc-ras.ru; ***e-mail: lov@isc-ras.ru*

Received January 15, 2021; revised February 1, 2021; accepted February 15, 2021

Abstract—The article presents a comprehensive approach to the investigation of the features of the chemical and supramolecular structure of pectin substances from plant tissues of the flax stem in relation to the manifestation patterns of the sorption properties of polyuronides with regard to theophylline, selected as the azaheterocyclic mycotoxin model. The preservation of the structure of the extracted pectin substances has been ensured using the methods of the enzymatic destruction of flax neutral polysaccharides and ultrasonic activation of the extraction processes. The methods of Fourier-IR spectroscopy, viscometry, IR spectrometry of pectin films, stationary sorption from the limited volume, and electron spectroscopy of solutions have been applied in the experimental studies. The analysis of the sorption research results has been carried out using the Boyd, Weber-Morris, and gel diffusion models, as well as the Lagergren and Ho and McKay kinetic models. The models of the polymer chain molecular structure and the spatial interaction between macromolecules in the sorption grain structure have been proposed based on the data on the chemical state of polyuronides. The effect of the structural arrangement of polyuronides on the equilibrium sorption level within the pH range of 2–6.5, on the characteristics of the external and internal diffusion limitation of the mass transfer, as well as on the sorption rate constant, and the limit sorption level of the biopolymer has been traced. The research results make it possible to predict the sorption binding of alkaloids by pectin substrates based on the data on the ratio of the forms of galacturonate units and to provide a comprehensive solution to the urgent tasks to optimize the feeding of ruminants, including the prevention of mycotoxicosis by numerous types of azaheterocyclic mycotoxins.

Keywords: flax plant tissue pectins, chemical state of galacturonate units, supramolecular structure of pectins, theophylline absorption, modeling of diffusion and kinetic parameters of sorption

DOI: 10.1134/S1070363221130399

INTRODUCTION

The chemistry and technology of pectin are undergoing a new round of rapid development. Along with the conventional areas of application of the biopolymer in the food and pharmaceutical industries, there is a growing interest to use its ability to various types of interactions to obtain new functionalized materials. In particular, the development of special modification methods ensures the production of self-stitched pectin hydrogels with silk fibroin, possessing a high mechanical strength and variable properties, which are of interest in bone tissue engineering [1]. The management of the structural organization of pectin hydrogels with chitosan and nanocrystalline cellulose makes it possible to obtain biofunctional injection materials for tissue engineering [2]. Pectin is used as a structuring additive in the composition of polyetherimide ultrafiltration membranes [3].

Increased attention is paid to issues related to the management of pectin substances properties directly in the structure of plant-based materials. Taking into account the expansion of the practical application areas of composite materials reinforced with flax fibers, studies of the cooperative effect of the pectin matrix in the fiber structure and the polymer binder in interfiber spaces are of great importance [4], as well as the influence of the conditions of flax stems microbiological processing on the properties of the obtained technical fibers and the formed composites [5].

Pectin substances are an important multifunctional component in the composition of fodder phyto-supplements. The development of physicochemical approaches to the solution of urgent tasks in the development of a fodder base for highly productive livestock farming is largely associated with the justification of methods for managing the set of adsorption interactions with the participation of polyuronides under the specific conditions of multistage digestive processes.

In particular, the organization of rational nutrition of ruminants is based on the fact that biochemical transformations of the fodder mass begin already at the first stage of its stay in the rumen and these processes make a predominant contribution to the provision of carbohydrate components [6, 7]. At the same time, the demand for amino acids is satisfied due to the later feed protein digestion in the intestine [8, 9]. A lot of interesting new data appear in studies dedicated to these processes.

The problem of protein protection from premature splitting is solved in various ways, including by search and introduction of herbal supplements with proteins, resistant to enzymatic effects of microorganisms developing in the rumen, into the diet [10–13]. The methods of protein thermal denaturation or chemical modification, for example, with formaldehyde, are applied [14–16]. There are recommendations to use amino acids in the chemically bound form [17, 18]. At the same time, experts note that the increased protein protection degree can lead to a decrease in the cattle productivity due to insufficient nitrogen nutrition for the development of the rumen microflora, as well as low assimilation of the transformed proteins in the acid digestion departments [19].

A compromise option can be provided by sorption methods of reversible binding of protein substances by compounds of polycationic and polyanionic nature [20], including the application of pectin-containing plant raw materials [21–23]. Taking into account the changing acidity degree in different organs of the ruminants' digestive tract, the influence of the medium pH value on the strength of proteins interactions with pectin substances is of great importance [24]. We have shown that in order to increase the adsorption capacity of phyto-supplements, it is important to ensure the release of pectins from the mesh structures of the binder in intercellular spaces and middle plates of the plant objects [25–28]. The revealed patterns have been embodied in specialized methods for enzymatic modification of flax materials, used in compositions with high-protein concentrates to ensure 85% resistance of protein substances to splitting by the rumen microflora [29]. The results are consistent with the recently published efficiency evaluation data on the use of flax-protein fodder supplements in vivo [30].

The methods applied to increase the completeness of utilization of the roughage fodder nutrients include silage under the influence of spontaneous microflora or biomodification with the use of selected microbial compositions [31, 32]. During these processes, as well as in case of violations of the fodder storage conditions, there is an increased risk of the biomass damage by mycotoxins—secondary metabolites of a number of microscopic fungi, posing a serious threat to both livestock and human health. There are more than 300 known varieties of toxic compounds of microbial origin, subdivided based on the special features of their molecular structure. The characteristics of the most widespread and dangerous substances are presented in reviews [33–35].

Along with the application of special physical and chemical fodder preparation methods for the prevention of mycotoxicosis, the most common preventive measure is the use of adsorbents. The sorbent is selected taking into account the polarity of the compounds to be neutralized [36, 37]. In particular, the aluminosilicates application efficiency has been confirmed with respect to polar substances, for example, aflotoxins. Activated carbon is better at binding hydrophobic mycotoxins, which do not contain polar groups, in particular, polycyclic aromatic compounds of the trichocene type. The scope of application of plant sorbents is associated with the activity of beta-glucans against compounds containing aliphatic or aromatic hydroxyls, such as zeralenone, fumonisins, and achrotoxins [38, 39]. Detoxification of the livestock, using pectin-containing citrus raw materials, has been demonstrated in tests in vivo [40].

On the territory of the Russian Federation, the agricultural fodder quality is evaluated taking into account the maximum permissible level (MPL) of mycotoxins, the parameters of which are regulated for a limited range of the most widespread and dangerous compounds [41]. For example, the MPL value for the aflotoxin content in plant fodder is 0.05 mg/kg. As a rule, the practically registered content of individual compounds of this

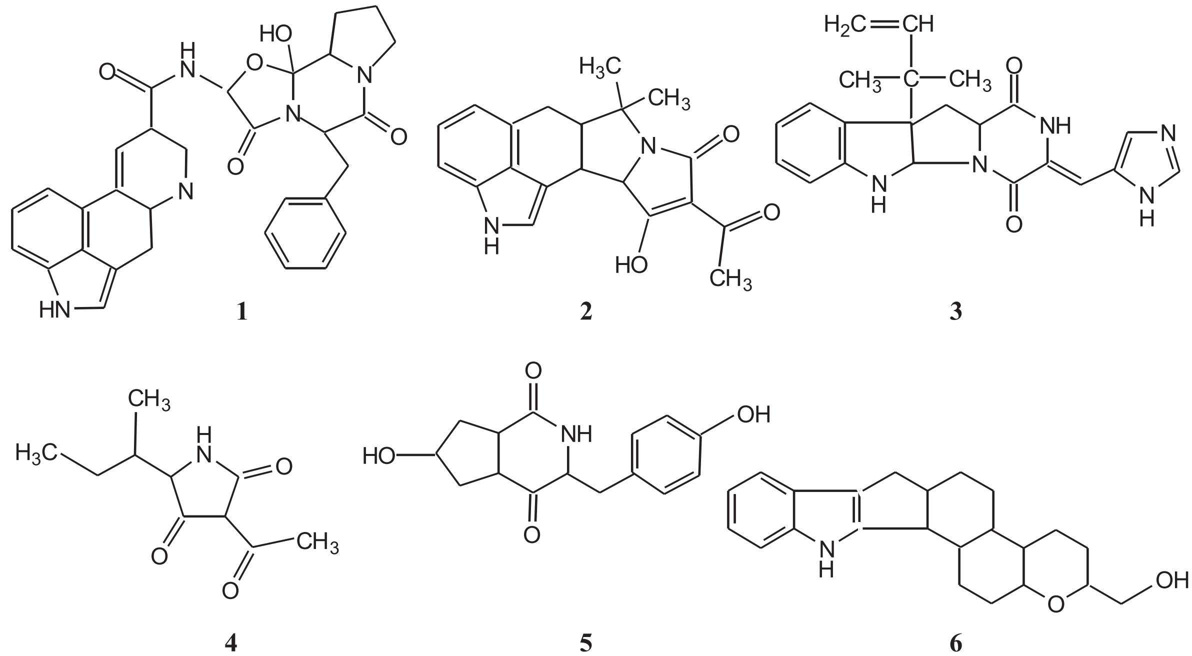

Fig. 1. Structural diagrams of mycotoxins from the group of heterocyclic alkaloids.

group is 1–2 decimal orders lower than the MPL. At the same time, it is known that the applied measures of protection against major toxins can be insufficient, as their effect is combined with the influence of other simultaneously present hazardous substances with possible manifestations of synergy [42]. In this regard, there is increased relevance of complex use of sorbents of different nature to ensure their complementary effects for the prevention of mycotoxicosis.

The function of an additional detoxifier of the animal body can be performed by pectin substances, demonstrating activity in relation to a wide group of azaheterocyclic compounds in the acidic parts of the digestive tract. The chemical structure of several representatives of the alkaloid group is presented in Fig. 1. Major mycotoxins include ergotamine (**1**), cyclopiazonic acid (**2**), and rokefortin (**3**), produced by widespread universal saprophytes of the *Penicillium* and *Aspergillus* genera. Plant fodder and silage are often affected by the metabolites of the *Alternaria* genus fungi, including tenuazonic acid (**4**) and macuzoline (**5**) [43]. A serious danger is presented by tremorgenic and neurotoxic indole-terpene derivatives of paspalin (**6**), considered in review [44].

The similarity of the compounds presented in the diagram is that they are poorly soluble in water and neutral aqueous systems; however, in an acidic environment they gain solubility and diffusion mobility due to the protonation of nitrogen atoms with a lone-electron pair. It is reasonable to expect that molecules of the protonated alkaloids can effectively interact with pectin substances in the composition of the stabilizing fodder supplement according to the method [29]. There are objective prerequisites for that, as having fulfilled their protein-protecting functions in the rumen and entering the main part of the stomach (abomasum) with a strongly acidic medium (pH of 1.5–2.5), pectins are freed from proteins as a result of suppression of the carboxyl groups dissociation. The pectins resume their activity when they enter the duodenum, at the entrance to which the pH level is 4.5 units, at the exit – 6.8 units. It is obvious that these parameters determine the practiced conditions for testing the binding capacity of enterosorbents in tests *in vitro* [45].

The length of the ruminants' duodenum is much greater than the length of the human organ (50 cm for goats and sheep, 120 cm for cows, and up to 200 cm for bulls and buffaloes). The duration of the digested fodder stay in this part of the cow's intestine does not exceed

30 min. The assessment of the sorption process kinetic characteristics will make it possible to substantiate the standards for introduction of pectin-containing phyto-supplements to prevent the absorption of mycotoxins in the subsequent intestinal sections and to reduce the load on the ruminants' physiological detoxification system.

Pectin compounds from various plant sources have significant differences in the proportion of galacturonate units with the unsubstituted carboxyl group, as well as in the methoxylated and calcium-pectate forms. The structure of pectins in flax materials also significantly varies depending on the genotype (selection variety) of the linen flax and the conditions of ontogenesis and processing of the plant raw material [46–49]. The necessity to analyze the specific manifestation of the pectin substances sorption activity in relation to nitrogen-containing mycotoxins is confirmed by the previously identified patterns of influence of the chemical structure of homogalacturonans on sorption binding of metal ions and polar organic compounds with differentiation of the contribution by various mechanisms of adsorption interactions [50, 51]. Taking into account the wide application of aluminosilicate sorbents for the prevention of mycotoxicosis, it is of great scientific and practical importance to model the sorption of alkaloids by binary polymer-inorganic systems, taking into account the previously identified enhancement of the mutual action of the components of pectin-montmorillonite complexes against inorganic and organic pollutants [52, 53].

The purpose of the performed studies was to identify the "composition–property" patterns in the description of the sorption kinetics of heterocyclic compounds of imidazole and pyrazole derivatives by pectin sorbents, taking into account the data on the specific features of the polyuronides structure in various plant tissues of the flax stem, separated with different types of flax processing by-products, to model the effectiveness of the binding of mycotoxins by flax-containing fodder supplements for ruminants.

EXPERIMENTAL

Materials. The model of azaheterocyclic mycotoxins was represented by a compound, consisting of a system of the pyrimidine and imidazole cycles with two common carbon atoms and belonging to the group of purine bases, namely 1,3-dimethyl-7*H*-purine-2,6-dione:

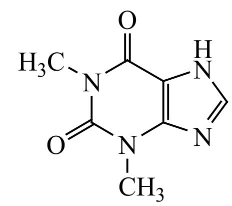

The trivial name of the compound is theophylline. It is applied as a pesticide and a medicine. According to the value of the median lethal dose, LD_{50} index (225 mg/kg), the substance belongs to the third hazard class (moderately hazardous substances), which allows it to be used in experimental chemical research. The pharmaceutical form of the drug was used in the work (manufactured by Valenta Pharm JSC, Russia).

The pectin substances under study were obtained from the following three types of by-products of the industrial processing of *Linum usitatissimum L.*: flax shive, tow, and flocks. The manufacturers are Korona LLC, Ivanovo, and L'nyanaya Manufaktura Kuzmina, Novosibirsk region.

When isolating pectin substances, the process of bio-splitting of the carbohydrate components of plant-based fodder in the ruminants' rumen was simulated using enzymes, catalyzing the hydrolysis of cellulose, xylans, and glucans without damaging the polyuronides [54]. The flax materials bio-treatment with CelloLux-F (manufactured by Sibbipharm Ltd., Novosibirsk) was carried out at the solution temperature of 40°C and the pH value of 7 for 6 h.

The pectin was extracted with hot (92°C) water under ultrasound exposure in accordance with the recommendations [55]. The treatment was carried out in the UZDN-2T disintegrator at a frequency of 22 kHz. The pectin precipitation was carried out by introducing 96% ethanol into the extract in a ratio of 1 : 3, the separated pectin coagulate was washed with 70 and 96% ethyl alcohol and dried at 60°C.

The preparation specifics of flax shive pectins included the initial extraction of water-soluble fractions with warm (40°C) water while stirring for 8 h.

As a comparison sample of an effective sorbent, an aluminosilicate drug was used, namely, Na-montmorillonite (Mt) of the Cloisite® Na brand by Southern Clay Products, Inc. (USA), chemically pure, with a cation-exchange capacity of 92.6 mg-eq/100 g.

To obtain bicomponent pectin-montmorillonite systems, the method to produce montmorillonite-starch composites was adapted [56]. Montmorillonite slurry was previously prepared in distilled water for swelling (Mt:water ratio was 70 : 30). Next, a weighed sample of the polyuronide powder form was mixed with the swollen clay mineral particles in a percentage ratio of 80 : 20 with treatment at the vibration mill (operating parameters of the unit: vibration frequency of the activator—50 Hz, vibration amplitude—180 μm, vibration velocity—158 mm/s, vibration acceleration—140 m/s^2, and the exposure duration—30 min). The resulting composite was dried at a temperature of 40°C for 1 h (vacuum drying at 66.5 kPa) with further exposure in the calcium chloride desiccator.

Instruments and methods of analysis. The identification of pectins was carried out using the IR-Fourier spectroscopy method. The IR spectra were recorded on the Vertex 80v infrared Fourier spectrometer by Bruker in the frequency range of 400–4000 cm^{-1} with the resolution of 2 cm^{-1}. The samples were prepared in the form of compressed tablets from the pectin and KBr powder mixture in a ratio of 1 : 150.

The analysis of the ratio of pectin galacturonate units in the unsubstituted, methoxylated, and calcium-pectate forms was carried out using the method of IR spectrometry of pectin films, based on the intensity measurement of the isolated band of stretching vibrations of the bond ν_{as}(C–OMe) at 1615 cm^{-1}, which characterizes the absorption of pectinates with mono- and divalent metal ions [57]. The experiment involves a cycle of operations in order to obtain modified preparations through successive chemical transformations of the monomers of free galacturonic acid and methoxylated units into the calcium pectate form [50]. The spectra were taken on the AVATAR-360 spectrophotometer in the transmission mode in the frequency range of 500–4000 cm^{-1}.

To determine the polymerization degree of tissue pectins, the preparations were pre-decalcified with 0.1 N NaOH solution for 1 h at room temperature. According to the data on the kinematic viscosity (η) of 0.1–1% pectin hydrogels, measured using Ostwald's capillary viscometer, the characteristic viscosity [η] was graphically determined based on the dependences of $\eta_{sp}/c = f(c)$ and $\ln((\eta/\eta_0)/c) = f(c)$.

The molecular mass (M_r) was calculated using the Mark–Kuhn–Houwink equation:

$$[\eta] = KM_r^a,$$

where K and a were coefficients, characterizing the interaction of the polymer with the solvent and the form of the macromolecule, $K = 1.1\times10^{-5}$; $a = 1.22$.

The polymerization degree was calculated according to the formula:

$$PD = M_r/M_{GA}$$

where M_{GA} = 194 g/mmol was the molar mass of galacturonic acid.

The analysis of theophylline sorption was carried out under static conditions from the limited volume at a temperature of 40°C and variable pH values of 2.0–6.5 created by phosphate buffer solutions. To obtain the sorption kinetic curves, 5 mL of 0.5% pectin solution and 20 mL of theophylline were placed in a series of measuring flasks to ensure the initial concentration (C_0) of the sorbate of 2 mM/L in the total volume of the solution. The number of samples in the series ensured consistent analysis at regular intervals (t) in the course of 120 min. For the analysis, the reaction mixture of the test sample was centrifuged for 10 min at 2000 rpm to separate the sorbent and determine the current concentration of theophylline in the supernatant (C_τ) using the electron spectroscopy method by its absorption at 270 nm on the UV/VIS spectrophotometer Unico 2800. The theophylline amount in the sorbent at the moment of time t (q_t, mmol/g) was calculated by the equation:

$$q_t = (C_0 - C_\tau)V/mM_T,$$

where M_T = 184 g/mol was the molar mass of theophylline; m was the mass of the weighed sample of the sorbent, g.

To analyze the sorption kinetic patterns, the Boyd [58], Weber–Morris [59], and gel diffusion models [60], as well as the Lagergren pseudo-first-order and Ho and McKay pseudo-second-order kinetic models were used [61–63].

RESULTS AND DISCUSSION

Characteristics of the studied flax substrates and polyuronide preparations. The flax materials used in the work are by-products at successive stages of the mechanical processing of raw materials for flax fiber production. Within the framework of this study, an important difference between the objects is that each of them predominantly contains pectins from different plant tissues of the flax stem.

Table 1. Mass fraction of polyuronides in flax materials under study and results of viscometric determination of their polymerization degree

Flax substrate	Pectin-containing tissue	Pectin symbol	Content in the substrate, wt %	Intrinsic viscosity, [η], cm^3/g	Molecular mass, M_r, kDa	Polymerization degree, *PD*
Shive	–	P_{MIGR}	4.0	1.15 ± 0.05[a]	12.9 ± 0.6[a]	67 ± 3[a]
	Xylem	P_{XYL}	3.6	23.67 ± 0.29	155.6 ± 1.9	802 ± 10
Tow	Parenchyma	P_{PAR}	6.3	3.07 ± 0.05	29.1 ± 0.5	150 ± 3
Flocks	Bast	P_{BAST}	5.4	10.79 ± 0.45	81.5 ± 3.4	420 ± 17

[a] For P_{MIGR} sample the values for the extracted product are indicated; for other samples—for individual macromolecules.

When processing the flax straw at a breaking machine, the inner, woody part of the stem is crushed. The main pectin-containing component in the separated flax shive particles is represented by the conductive tissues of xylem. In the flax scutching process, the fibrous bundles are separated from the peripheral layer of the stem, which is facilitated by microbiological destruction of its components in the process of meadow spreading or, as it is commonly called, dew retting of flax raw materials. The by-product of scutching is tow, which contains tangled non-spun fibrous complexes with the remains of poorly cleaved parenchyma cells, surrounding the bast bundles. Flocks are the waste of processing at hackling machines and tow shakers. This material predominantly contains a down fraction of short flax fibers with pectins in the cell wall of the fibers and middle plates of the bast bundles.

Thus, we have classified and designated preparations of the isolated polyuronide substrates under comparison as the bast pectin (P_{BAST}), the parenchyma pectin (P_{PAR}), and the xylem pectin (P_{XYL}). To generalize this group of samples, we will use the name of tissue pectins. At the same time, during the flax shive preparation process, it has been possible to identify the presence of water-soluble polyuronides in the substrate, which cannot be a component of the xylem cell walls, as in the plant ontogenesis process, the nutrients and the absorbed soil moisture are transferred through the conductive tissue channels. Apparently, the appearance of this fraction in the shive is associated with the splitting of pectin substances in the peripheral layers of the stem under conditions of many days of dew retting. Due to the condensation of moisture in the channels of the xylem tracheal elements, there is a possibility for the diffusion of water-soluble products of the pectin destruction with the accumulation of the migrating polyuronides fraction (P_{MIGR}).

The data in Table 1 confirm the assumption that the fraction of migrating pectins is an oligomeric product with a small number of interconnected monomer units. Moreover, its amount in the substrate exceeds its own content of pectins in the xylem cell wall.

The largest amount of pectin substances is found in flax tow samples; however, the average value of their molecular mass is almost 3 times lower as compared to the bast pectins. Apparently, these data reflect the successful solution of the flax dew retting tasks to ensure efficient maceration of the stem bark layer without damaging the fibrous bundles. The highest polymerization degree is characteristic of the P_{XYL} preparation polyuronides, which is associated with the structural features of the xylem. As known [64], the channels of the tracheal elements in the xylem are formed by elongated cells, the death of which leads to the formation of a through internal cavity. The radial dimensions of the channels (15–30 μm) by far exceed the wall thickness (2–5 μm), which makes the increased length of the polyuronide macromolecule necessary to bind the polymer chains and consolidate the structure of the lignocellulose complex.

The identification of the obtained pectin preparations was carried out based on the set of the vibration processes characteristic bands recorded by the Fourier-IR spectroscopy method. The spectrograms taken in the transmission mode are presented in Fig. 2.

The recorded set of the main absorption peaks corresponds to the published data on the characteristic frequencies of the vibration processes for a variety of covalent bonds in the structure of the pectin substances macromolecule [65]:

—1720 cm^{-1}, fluctuations of C=O bonds in non-esterified carboxyl groups;

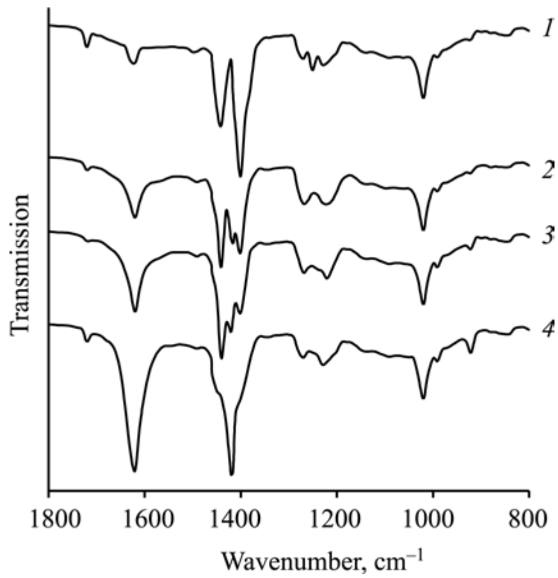

Fig. 2. IR Transmission spectra of pectin substances preparations from flax substrates: (*1*) P_{MIGR}; (*2*) P_{BAST}; (*3*) P_{PAR}; and (*4*) P_{XYL}.

—1420 and 1620 cm^{-1}, symmetric and asymmetric stretching vibrations of carboxyl bonds with metal ions ν_s, ν_{as} (C–OMe);

—1440 cm^{-1}, internal deformation asymmetric vibrations of the methyl group in carboxyl δ_{as}(O–CH$_3$);

—1400 cm^{-1}, stretching vibrations of the C–OH bond in carboxyl ν(C–OH);

—1020–1010 cm^{-1}, stretching vibrations of pyranose rings ν(C–C)(C–O);

—990 cm^{-1}, deformation vibrations of carboxyl δ(C–OMe); and

—920 cm^{-1}, pendulum vibrations of methyl in the ester group ρ(O–CH$_3$).

Table 2. Results of analysis of the chemical structure of polyuronide substrates

Pectin	Fractional content of galacturonate units forms, units		
	GH	*GM*	*GC*
P_{MIGR}	0.50	0.44	0.06
P_{BAST}	0.30	0.55	0.15
P_{PAR}	0.22	0.58	0.20
P_{XYL}	0.27	0.37	0.36

The intensity of the main absorption bands for the obtained flax pectins varies significantly. In the P_{MIGR} spectrum, the greatest intensity is demonstrated by the peaks at 1400 and 1720 cm^{-1}, corresponding to the stretching vibrations of non-esterified carboxyl groups, against a significantly lower intensity of the carboxyl vibrations in the calcium-pectate form (1620 cm^{-1}). On the contrary, in the P_{XYL} spectrogram, the most pronounced peak is at 1620 cm^{-1}, characterizing the absorption of pectinates with calcium ions.

At the same time, the pectins spectra do not allow us to quantitatively characterize the content of galacturonate units with a different status of the carboxyl group. This fact results from the impossibility to isolate the vibration bands of ν(C–OH) and δ_{as}(O–CH$_3$) in unsubstituted and methoxylated carboxyl from the complex superposition of the overlapping vibration processes in the frequency range of 1350–1450 cm^{-1}. The analysis of the methoxyl group number by the absorption bands maxima of the stretching vibrations of the ester bond ν (C–O–C) at 1272 and 1223 cm^{-1} is also impossible due to the overlapping absorption bands of the deformation vibrations of the pyranose rings C–H bond and the O–H bond of the alcohol hydroxyl group in this region.

The isolated band is represented by the peak of asymmetric stretching vibrations of the C–O bond in the pectate at 1620 cm^{-1}. The assessment of the intensity change of this stretching vibrations band forms the basis for the applied method to determine the fractional content of galacturonate units in the unsubstituted, methoxylated, and calcium-pectate forms. The method is implemented through successive transformations of the free non-esterified and methoxylated forms of galacturonic acid into calcium pectate with registration of the specific absorption increase at a frequency of 1620 cm^{-1} by the method of IR spectroscopy of polymer films.

Table 2 compares the pectin preparations under study by the content of galacturonate units with carboxyl groups in the unsubstituted (*GH*), methoxylated (*GM*), and calcium-pectate (*GC*) forms. The results are presented in share terms to the total number of galacturonate units.

As can be seen, the compared pectin preparations differ significantly with regard to the number of *GH* units, determining the chemisorption potential of polyuronides in relation to positively charged substances. Usually, when characterizing the sorption capacity of pectins, attention is paid only to their methoxylation degree, as esterification of carboxyls reduces the biopolymer reactivity, especially in an acidic medium [66]. The replacement of calcium ions in sorption processes is possible only by cations, providing a higher stability of the pectinates [67].

Under the conditions of sorption interactions with the participation of polyuronides that we have modeled, the *GC* form is not an indifferent witness and is able to affect the chemisorption activity of the substrate. It should be taken into account that after being freed from the digested fodder fiber, the pectins are transferred to the colloidal state. As known, the content of Ca^{2+} ions in the polymer has a decisive effect on the gelation, structure, and stability of pectin gels [68, 69].

A unit in the calcium-pectate form cannot appear in the polymer chain individually. There necessarily has to be an unsubstituted unit in another polyuronide macromolecule at a distance sufficient for interaction. The chains crosslinking will be stable only in case similar bridges occur at the adjacent units, which leads to the appearance of a stable "egg-box" conformation formation [70], the diagram of which is presented in Fig. 3a.

Taking into account the spatial orientation of glucopyranose cycles, the *GC* form can only appear in alternation with other monomer unit varieties. The carboxyl group in the adjacent cycles has to be predominantly unsubstituted, which makes it possible to embed Ca^{2+} ions on any side of the macromolecule, depending on the location of the nearby chain with a complementary fragment. This ensures a possibility of formation of multilayer "egg-box" structures [71], which is apparently realized only at high concentrations of pectin substances.

The repetitive crosslinks number in natural pectin blocks, as a rule, does not exceed four [72, 73], the minimum number is two. Therefore, the option with one *GH* unit in the neighborhood with several *GM* units, presented in Fig. 3b, does not suggest the Ca^{2+} ion absorption and reflects possible alternation of the subunits in the structure of branched domains.

Based on above postulates, the supramolecular structure of the compared polyuronide samples has been modeled in accordance with the data in Table 2. For the P_{MIGR} sample, in accordance with the experimental determination conditions, the value of PD = 67 (see Table 1) is a characteristic not of the individual polymer chain, but of the structure fragment in which a group of macromolecules is united by a certain number of crosslinking blocks. In this case, there is only one possible option of the structural combination of units, in which two oligomeric chains are connected by a single "egg-box" block, consisting of two cells in full accordance with the scheme in Fig. 3a. In this case, the four branches contain a total number of 30 *GM*–*GH* paired repetitions.

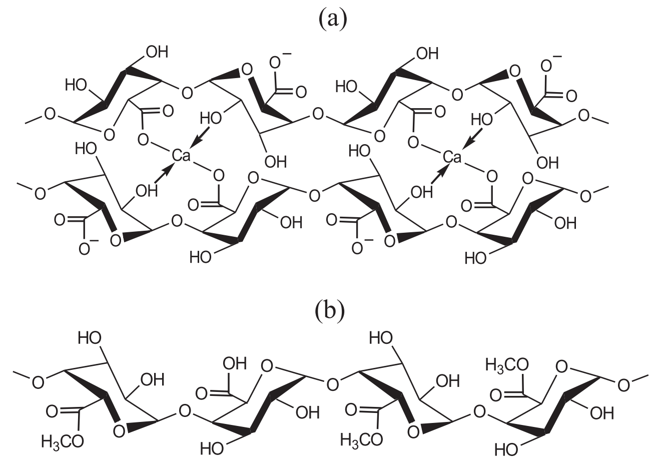

Fig. 3. Diagram of the "egg-box" conformational formation with participation of the calcium-pectate form (a) and chain fragment of branched domains (b) in the pectin structure.

For tissue pectins, the following statistically probable scenarios of formation of the crosslinking blocks and the branched part have been determined, taking into account the established values of the polymer chain length for individual macromolecules:

—P_{PAR} – taking into account PD = 150, the aggregate composition of $GH_{33}GM_{87}GC_{30}$ units has the following grouped distribution: $[(GC_2GH_2)(GM_7)]_{15}GH_3$; i.e. each macromolecule passes through 15 blocks with two *GC* units alternating with two *GH* units, the blocks are separated by branches of seven *GM* units, in every fifth branch there is one *GH* unit;

—P_{BAST} – when PD = 420, the total composition of $GH_{126}GM_{231}GC_{63}$ gives the following distribution: $[(GC_3GH_3)(GM_{11}GH_3)]_{21}$, i.e. the macromolecule 21 times contacts with the adjacent chains in blocks with three *GC*-*GH* pairs, whereas in the branches three *GH* units correspond to eleven *GM* units;

—P_{XYL} – for PD = 792, the composition of $GH_{216}GM_{288}GC_{288}$ units gives the following distribution: $[(GC_4GH_3GM)GM_3]_{72}$; i.e. each macromolecule participates in 72 blocks with four *GC* units, between which there are three *GC* units and one *GM* unit on the edge, whereas the ultrashort flexible segments consist of

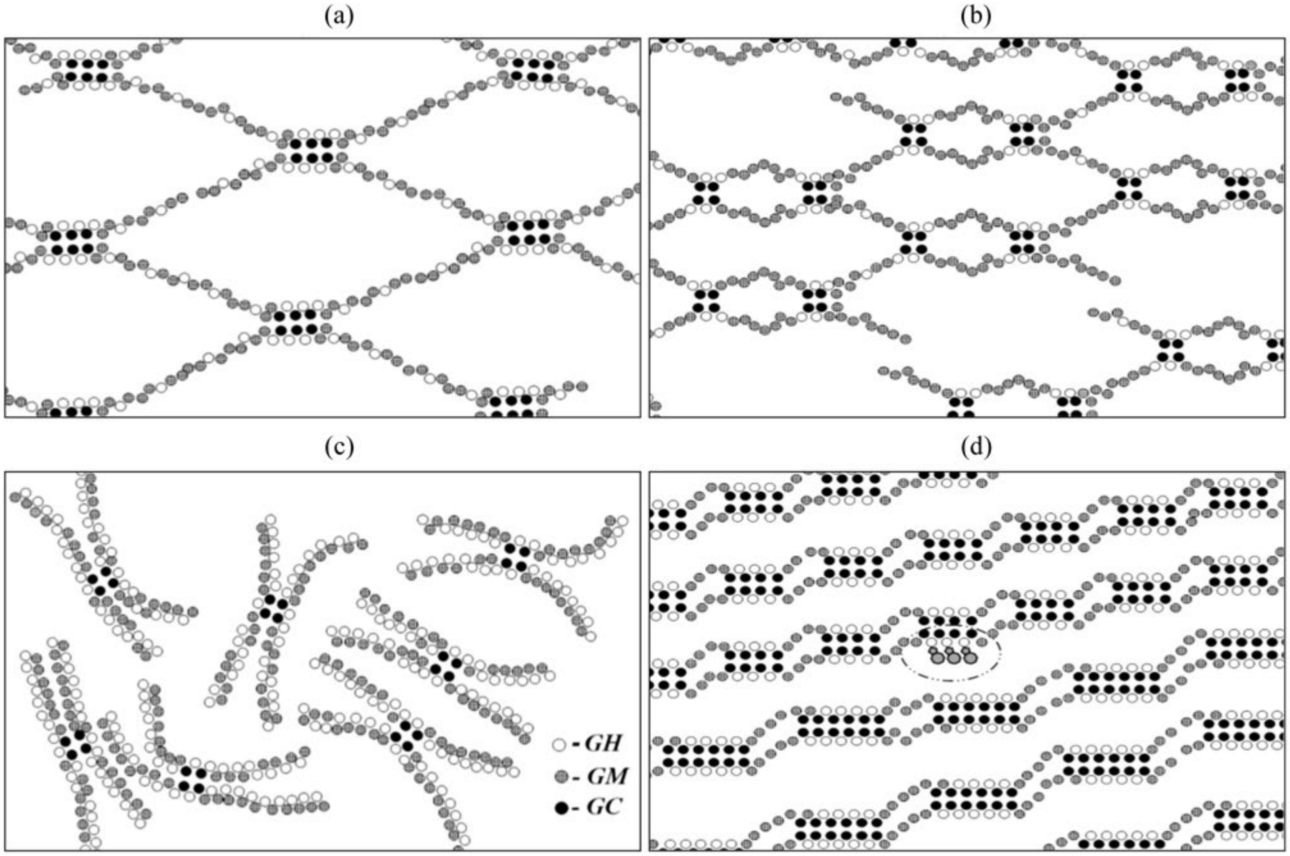

Fig. 4. Structural arrangement model of polyuronide gels in samples under study: (a) P_{BAST}, (b) P_{PAR}, (c) P_{MIGR}, and (d) P_{XYL}.

three *GM* units. An increase in the flexible segment length is possible only in case their number is reduced, i.e. due to a greater number of *GC* units in the composition of the "egg-box" formations. For example, for $PD = 812$, the composition of $GH_{216}GM_{312}GC_{288}$ units can be distributed into 48 blocks with six *GC* units: $[(GC_6GH_6GM)GM_5]_{24}\cdot[(GC_6GH_4GM_2)GM_5]_{24}$. However, even in this scenario, the branches contain only five *GM* units.

The mutual arrangement of chains in the polyuronide samples under study is shown in Fig. 4.

The following assumptions are made when constructing the models. First of all, they are related to the two-dimensional representation of the macromolecular chains interconnections, simplifying the actual 3d-arrangement of polymer networks. This version can be considered as a fragment of a single mesh layer, from which macromolecules can move to the adjacent parallel layers. To simplify, the number of *GC* units in the crosslinking blocks is assumed to be constant and multiple of the experimental value of the content of this form in the polymer. The number of monomer units in flexible segments between seals is also proportionally distributed. It is obvious that fluctuations in these parameters are possible; however, they balance each other. The diagrams reflect the statistically averaged distribution of the pectin structural elements in plant tissues. Finally, in the accepted version, the polymer structures are formed by homogalacturonane macromolecules. For real pectin substances, 2–4% of α-rhamnose residues have to be included into the diagrams [74]. The lateral branches from the rhamnose units will be oriented in the orthogonal direction, in parallel with the location of cellulose fibrils and hemicelluloses, so they do not affect the formation of the crosslinked mesh structure.

The presented diagrams make it possible to visualize the difference of the objects, hiding behind the numerical information on the ratio of the galacturonate unit forms (Table 2). It becomes clear that with an increase in the *GC* form content, the total number of units involved in blocks with a high-density crystal structure proportionally doubles. In this case, as a rule, the *GH* unit is a companion of the *GC* unit. The length of the flexible segments is symbatically reduced, which will affect the polymer swelling in water and the density of the formed hydrogels.

The largest sizes of branched domains in the P_{BAST} sample determine the hyperelastic properties of gels formed by flax fiber pectins that have been noted by experts [75]. The differences in the arrangement of mesh structures in comparison with the P_{PAR} preparation are quite natural, as in the bast, the polyuronide macromolecules have to bend around and hold together cellulose fibrils and lignocarbon formations with relatively large transverse dimensions. In the thin-walled parenchyma cells, pectin substances combine less thick bundles of the ordered hemicellulose macromolecules into carbohydrate-protein complexes.

It is obvious that after the destructive effect of microorganisms under the flax dew retting conditions, the structure of the bark layer pectins is significantly defragmented. This fact is illustrated by the gaps between the branched domains of the P_{PAR} preparation in Fig. 4b. It is quite logical that the fragments that have fallen out of the integral picture of the mesh formations are the shortened residues of P_{MYGR}, presented in Fig. 4c. The high density of *GH* units in the P_{MYGR} branches determines the complementarity of the site for the glucoside bond breaking under the action of pectinases in the flax dew retting processes, as well as the hydrate shell formation, ensuring the diffusion redistribution of the fermentation products deep into the stem.

Figure 4c shows both versions of the crosslinking blocks layout in the P_{XYL} preparation. As can be seen, variations in the number of the grouped *GC* units cause no fundamental changes in the nature of the polymer chains arrangement. The highly ordered structure of the P_{XYL} preparation is related to the high density of the substance in the xylem cell walls, which is associated with the distinctive features of the flax stem morphology. In its structure, there are no wood fibers (libriform), which provide the necessary level of strength to tissues in woody plant varieties. Therefore, unlike the majority of herbaceous plants, the flax xylem performs not only conductive, but also mechanical functions. The abnormally high degree of the xylem lignification is genetically predetermined in order to provide the flax stem with a sufficient level of strength [76, 77]. The walls of the tracheal elements are permeated and bound by spiral-shaped lignin formations. The stepped displacement of crosslinking blocks, shown in Fig. 4d, reflects the ability of polyuronides to follow the lignin spiral. In this case, the ribbon-like paired grouping of polymer chains is apparently more justified than the creation of mesh structures with transitions of macromolecules from one branched domain to another. It is facilitated by the small length of the flexible segment and the mutually ordered arrangement of sections with a favorable combination of monomer units for the formation of multiple inter-chain crosslinks in two adjacent macromolecules, the biosynthesis of which occurs together during the xylem cell growth. In this case, pectin substances are maximally capable of providing, along with lignin, an increase in the strength of the xylem cell walls, braiding and sealing the longitudinally located cellulose fibrils.

After the destruction of neutral polysaccharides in the process of pectins separation from flax raw materials, the mesh structure of the polyuronides is preserved not only in the resulting model preparations. In the same form, pectins are released in the digestive tract of ruminants and can take part in the ongoing absorption processes. It follows from the data of Fig. 4 that all the pectin samples under comparison have no fundamental restrictions for 100% participation of galacturonate *GH* units in interactions with theophylline molecules, simulating the binding of toxic alkaloids. Even units involved in the formation of “egg-box” blocks retain their ability for chemisorption binding of theophylline molecules, as reflected by symbols circled by a dash-dotted oval line in Fig. 4c.

In reality, as shown in Fig. 5a, theophylline molecules do not experience steric restrictions for interactions with ionized carboxyl groups in each paired repetition of polyuronide units, while fixing their position by a hydrogen bond with a secondary hydroxyl in the adjacent galacturonate unit.

The natural regulator of this process is the degree of the carboxyl groups dissociation, which, on the one hand, determines the number of reactive groups, and, on the other hand, affects the density of the hydrate shell around the polymer chain. In this regard, the optimum acidity in the cationic sorbates binding processes greatly varies from one researcher to another [78–83], depending on the

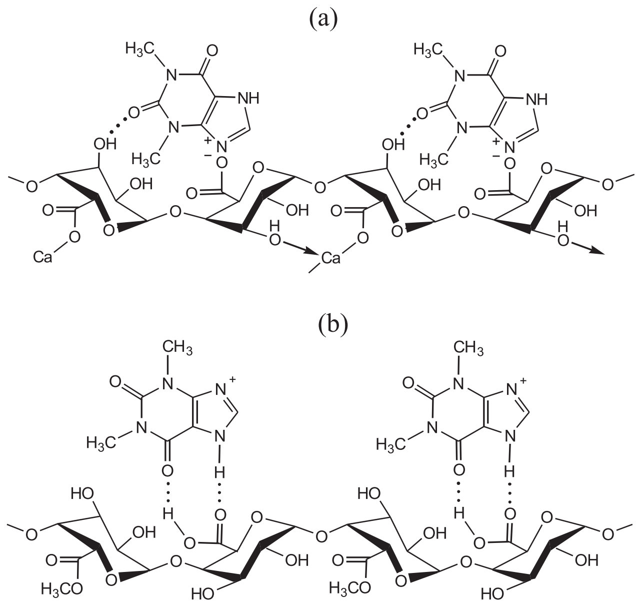

Fig. 5. Schemes of theophylline molecule absorption interaction with polyuronide in (a) moderately acidic and (b) strongly acidic media.

charge density on the surface of the sorbed particle and the pectin substrate type.

When the dissociation of unsubstituted carboxyl groups in a strongly acidic medium is suppressed, the absorption of theophylline is, apparently, also possible due to the formation of hydrogen bonds according to the scheme presented in Fig. 5b. Such interactions can occur, in particular, when the digested biomass stays in the main stomach of ruminants, where the pH level is from 1.5 to 2.5 units. It is evident that this form of binding will be fragile and reversible; however, it can stimulate the sorbate external diffusion stage and facilitate stronger binding at the increased pH value in the duodenum area.

A natural obstacle to the binding of alkaloids in a strongly acidic medium can be the approaching sections of the spatial grid of polyuronides with the appearance of multiple hydrogen bonds directly between undissociated carboxyl groups in units of the adjacent chains. In this connection, it is of interest to study the effect of the structural arrangement of mesh domains on the sorption capacity of the compared polyuronide samples not only for moderately and slightly acidic media, but also for strongly acidic solutions.

Patterns of theophylline absorption by flax pectins. *Influence of the medium acidity.* In the systems under study, it is necessary to take into account the multifactorial influence of the acidity level on the state of the components and the nature of the ongoing interactions. Figure 6 compares the values for two-hour sorption of the model alkaloid by pectin preparations in buffer systems with the pH level from 2.0 to 6.5 units at a temperature of 40°C.

The preparations demonstrate the highest level of sorption activity at the pH of 3.5. The dissociation of carboxyl groups in pectin and the protonation of the heteroatom in the imidazole cycle of theophylline create conditions for spontaneous chemisorption interactions. The sorption increment, observed under these conditions, during successive transitions from P_{PAR} to P_{MIGR} (see Fig. 6a), is proportional to the increase in the fractional content of galacturonate units in the GH form (see Table 2):

$$\Delta q = 1.4147GH,\ R^2 = 0.993.$$

If the calculated level of the substrates sorption potential Q_{max} is determined based on the possibilities to bind theophylline molecules by the whole set of unsubstituted carboxyl groups in a ratio of 1 : 1, then the diagram in Fig. 6b can reflect the completeness of utilization of the internal capabilities of the compared substrates. In this interpretation, it can be seen that the achieved degree of sorption (q_{120}/Q_{max}) is determined not only by the number of sorption centers, but also by their availability.

It is right to assume that even under the maximum efficiency conditions at the pH of 3.5, not all carboxyl groups in GH units are dissociated. At the same time, under the same conditions, the dissociation constant should have an equal value for all pectin samples. Consequently, there are obstacles for sorption interactions, which are most strongly manifested for the P_{PAR} and P_{BAST} substrates.

The comparison of results with our model ideas about the structure of pectin hydrogels (see Fig. 4) makes it possible to suggest that the increased resistance to embedding of theophylline in the mesh structure of the P_{PAR} and P_{BAST} preparations can be related to the screening of adsorption centers under the influence of numerous surroundings from the adjacent methoxylated units with specific structuring of water molecules in the shell of the hydrophobically hydrated methyl group. The basis for the hypothesis is a satisfactory correlation

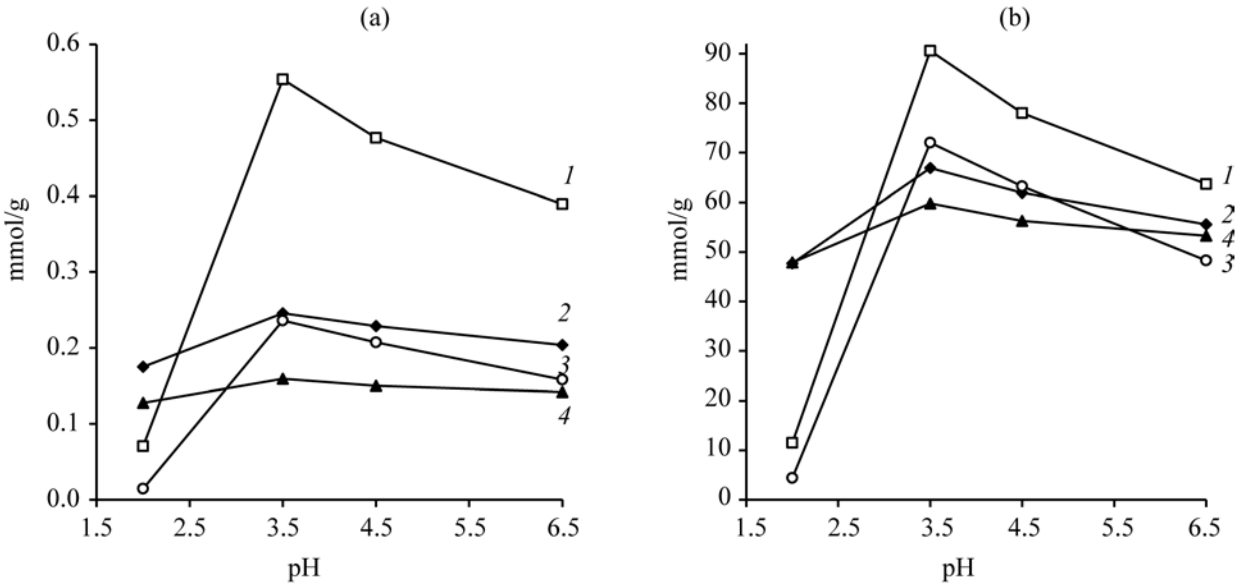

Fig. 6. Influence of pH on theophylline sorption by pectin preparations at 40°C for 120 min (a) and relative realization of the substrates sorption potential (b): (*1*) $P_{\rm MIGR}$; (*2*) $P_{\rm BAST}$; (*3*) $P_{\rm XYL}$; and (*4*) $P_{\rm PAR}$.

between the indicator of the sorption potential realization degree at the pH of 3.5 and the ratio of monomer units in the *GH* and *GM* forms in the polyuronides:

$$\frac{q_{120\,(\rm pH\,3.5)}}{Q_{\max}} = 40.241 + 44.156\frac{GH}{GM},\ R^2 = 0.9939.$$

It is significant that the free equation term almost coincides with the value of the $q_{120}/Q_{\max}$ indicator for the $P_{\rm PAR}$ и $P_{\rm BAST}$ preparations at the pH of 2. The equal absorption capacity of these substrates in a strongly acidic medium is consistent with the ideas about the equal availability of *GH* units in their mesh structure for the interaction with theophylline according to the scheme, presented in Fig. 5b. In this case, the remote location of macromolecules in branched domains manifests itself as a positive factor, preventing mutual orientation of sections with unsubstituted units and association of chains with the formation of hydrogen bonds between the atoms of carboxyl groups:

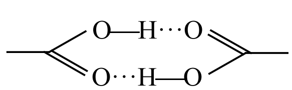

The diagrams in Figs. 4c and 4d demonstrate the structural predisposition of the $P_{\rm MIGR}$ and $P_{\rm XYL}$ hydrogels to self-association in a strongly acidic environment, which has to impair their ability to bind theophylline. The dramatic reduction of sorption by these preparations at the pH of 2 demonstrates the correctness of the assumptions about the substrates behavior, validity of the chosen approach to the system description and to the identification of levers to control the processes.

With an increase in the pH level to 4.5 and 6.5 units, the carboxyls ionization constant cannot go down. However, declining branches are observed on the graphs for all preparations (Fig. 6). The sorption reduction rates progress in the series: $P_{\rm PAR} \rightarrow P_{\rm BAST} \rightarrow P_{\rm XYL} \rightarrow P_{\rm MIGR}$. In the same sequence, there is an increase in the number of *GH* units embedded in the segments of their multiple alternations with other monomer forms. For tissue pectins, such segments are represented by chain sections in crosslinking blocks. In the $P_{\rm MIGR}$ preparation, the entire oligomeric segment of the chain falls under this criterion; however, the most important area is the "egg-box" cells branches.

The specificity of such segments is associated with sealing of the hydrate shell around the ionized carboxyl. In the presence of several dissociated *GH* units in the adjacent structural cells, the hydrate shells of carboxyls affect each other and are additionally compressed. In this

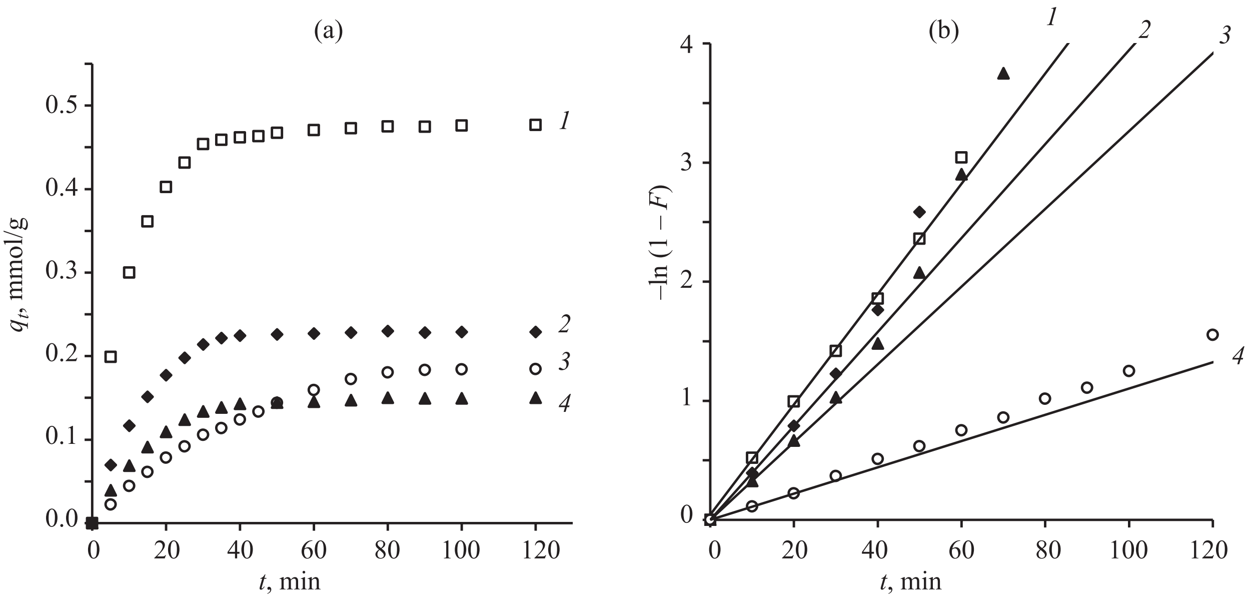

Fig. 7. Experimental dependencies of theophylline absorption by pectin preparations at pH of 4.5 (a) and their analysis in the boyd diffusion model coordinates (b): (*1*) P_{MIGR}; (*2*) P_{BAST}; (*3*) P_{XYL}; and (*4*) P_{PAR}.

regard, the appearance of a new dissociated group in the segment can lengthen (unite) the areas of the compacted hydrate environment of the polymer, creating an obstacle to the interaction of theophylline with the sorption center.

The number of N units in segments with a regular alternation of the *GH* form in the studied pectin samples increases in the row: $P_{\text{PAR}} - 4$, $P_{\text{BAST}} - 6$, $P_{\text{XYL}} - 8$ (or 12), and $P_{\text{MIGR}} - 17$. The dynamics of changes in the indicator N correlates with a decrease in the value $q_{120}/Q_{\max}$ at an increase in the pH value from 3.5 to 4.5 units. Moreover, the comparison of correlation ratios for alternative versions of formation of the "egg-box" structure in the P_{XYL} pectin makes it possible to give preference to a more elongated form of blocks with six crosslinks, as in this case the complete linearization of results is achieved as follows:

$$N(P_{\text{XYL}}) = 8; \frac{q_{120\,(\text{pH}\,3.5)} - q_{120\,(\text{pH}\,4.5)}}{Q_{\max}} = 1.541 + 0.678N,\ R^2 = 0.9094,$$

$$N(P_{\text{XYL}}) = 12; \frac{q_{120\,(\text{pH}\,3.5)} - q_{120\,(\text{pH}\,4.5)}}{Q_{\max}} = 0.748 + 0.69N,\ R^2 = 0.9984.$$

Thus, taking into account the parameter of the fodder mass acidity in the ruminants' duodenum, it can be assumed that under real conditions it will not be possible to ensure the optimal mode of sorption binding of azaheterocyclic mycotoxins with pectin substances of the flax component of fodder supplements. The 6–13% reduction from the level of realization of the pectins sorption potential at the pH of 3.5 can be associated with the structural features of the close hydrate environment of the sorption centers. Taking into account the obtained results, it is reasonable to start the analysis of kinetic dependencies and the identification of the key mechanisms of theophylline sorption by hydrogel preparations of pectins with primary differentiation of the internal and external diffusion limitation in the chemisorption process.

Analysis of the diffusion models of theophylline transfer in the colloidal system of flax pectins. The sorption experiments have been performed using highly

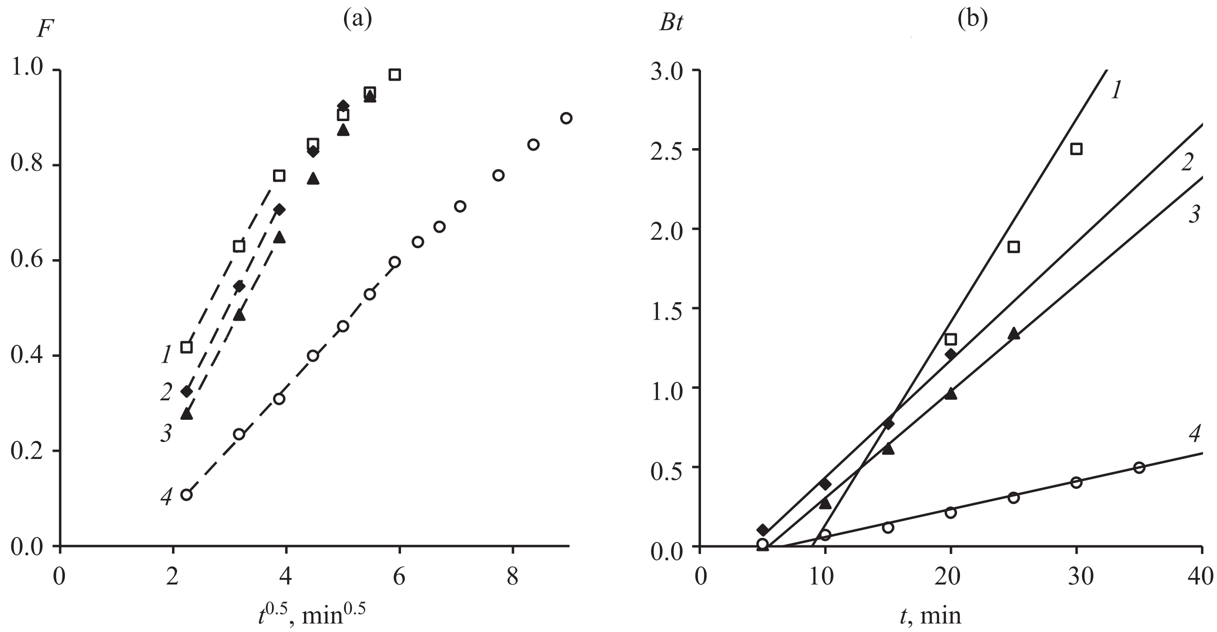

Fig. 8. Interpretation of kinetics of theophylline sorption by pectin samples in the weber-morris model (a) and the gel diffusion model (b) coordinates: (*1*) P_{MIGR}; (*2*) P_{BAST}; (*3*) P_{XYL}; and (*4*) P_{PAR}.

diluted (0.1%) solutions of pectin preparations, which is comparable to the actual level of pectins concentration in the volume of digested fodder biomass. After the dissolution of the P_{PAR}, P_{BAST}, and P_{XYL} powder substrates in water and their preliminary exposure for 20 min, microheterogenic systems are formed, represented by a suspension of swollen particles, the structure of which is preserved due to numerous crosslinks of polymer chains. In the P_{MIGR} solutions, the presence of the dispersed phase with a particle size of 35–40 nm is also registered by the dynamic light scattering method. Therefore, as in cases of solid-phase sorbents, the mass transfer process should be divided into the external diffusion to the particles surface and the internal diffusion in the structure of the swollen polyuronide.

Figure 7 shows the experimental kinetic curves of theophylline sorption at the pH of 4.5 and their graphical interpretation in the framework of the Boyd diffusion model, applied to characterize the sorption processes limitation scenarios by the external diffusion mass transfer stage [58, 84]. In this case, the dynamics of changes in current values of the amount of the bound sorbate q_t should be linearized in the coordinates—log (1–*F*) from *t*, where *t* means time, *F* is the equilibrium degree in the system, calculated based on the ratio of the current and equilibrium sorption values as follows: $F = (q_t/q_e)$.

The Boyd transformations adequately describe empirical data only when the required level of the determination coefficient ($R^2 > 0.9$) is provided; however, the compliance with this condition is often demonstrated by means of covering the regions of damped sorption and sorption equilibrium [85]. The results presented in Fig. 7b for the studied systems indicate that in the intensive sorption areas, the experimental values (points) quite quickly deviate from the vectors, uniting the first groups of values with the origin of coordinates and reflecting the external diffusion influence. For structured tissue pectins, the external diffusion inhibition manifests itself only during the first 10 min, when the binding of the sorbate occurs at relatively accessible adsorption centers. At later stages, the sorption process does not depend on the diffusion replenishment of the sorbate in the near-surface layer of the solution. Apparently, it is natural that the sorption dependence on the mobility of theophylline in the external environment has a more pronounced manifestation for the P_{MIGR} sample. However, even in this system, the correlation is broken 20 min after the sorption starts when less accessible galacturonate units, adjacent to the interchain crosslinking block, begin to participate in the sorbate binding (see Fig. 4c).

Figure 8 presents grouped results of the analysis of kinetic dependencies with the application of models,

Table 3. Kinetic parameters of the applied diffusion models of theophylline sorption by pectin preparations at 40°C and pH of 4.5

Pectin	Weber–Morris Model diffusion rate constant, mmol g^{-1} $min^{-0.5}$		Gel diffusion model	
	k_{D1}	k_{D2}	kinetic coefficient, $B\times10^3$, s^{-1}	effective diffusion coefficient, $D\times10^{11}$, m^2 s^{-1}
P_{XYL}	0.0267	0.0217	0.292	0.266
P_{PAR}	0.0322	0.0261	1.120	1.022
P_{BAST}	0.0511	0.0406	1.233	4.500
P_{MIGR}	0.0939	0.0461	1.942	0.0000279

taking into account the intradiffusion mechanism of the sorption process limitation. The conventional Weber–Morris model is considered by many experts as an option for multilinear description of the mass transfer with a mixed diffusion mode of limiting stages [86, 87]. The characteristic of the intradiffusion limitation is given by the empirical data linearization at a section with the substrate saturation degree F exceeding 0.5. Figure 8a shows options for division of the results into two linearized regions, which, according to the authors [88], make it possible to compare the kinetic characteristics of the external and internal diffusion stages, using the value of the diffusion rate constant k_D (mmol $g^{-1}min^{-0.5}$), included in the Weber–Morris model equation:

$$q_t = k_D t^{0.5} + C.$$

The value of k_D is determined taking into account the slope angle tangent of the corresponding section and the equilibrium sorption value q_e achieved in the experiment.

The application of the gel diffusion model makes it possible to determine the mass transfer kinetic parameters included in the Boyd equation for the intradiffusion sorption limitation [60]:

$$F = 1 - \frac{6}{\pi^2}\sum_{n=1}^{\infty}(1/n^2)\exp(-D\pi^2 n^2 r^{-2} t),$$

where $D\pi^2 r^{-2} = B$ is the kinetic coefficient, s^{-1}; D is the effective diffusion coefficient, m^2 s^{-1}; r is the average radius of the sorbent grain, m; and n – are natural numbers from 1 to infinity.

The construction of the dependencies $Bt = f(t)$ presented in Fig. 8b is carried out by transforming the $F = f(t)$ ratio, using reference data to determine the value of the product Bt [89]. For the P_{MIGR} preparation, the analysis is carried out for a time interval of 20–30 min, at which a sharp slowdown in sorption has been observed (see Fig. 8a) when the substrate saturation degree F has exceeded 0.75. For tissue pectins, the results in Fig. 8b are satisfactorily described by linear functions within the entire time range, which confirms the adequacy of the intradiffusion limitation assessment within the framework of this model and makes it possible, based on the approximating dependency angle, to determine the values of the characteristic parameters of the kinetic coefficient B and the effective internal diffusion coefficient D.

The data analysis results, presented in Fig. 8, are summarized in Table 3 and make it possible to quantitatively compare the effect of the structural arrangement of pectin substances on the specific character of the sorbed theophylline diffusion transfer.

It should be noted that the constant k_{D1} is not an absolute characteristic of the sorbate diffusion mobility in the solvent, as its value also depends on the kinetic parameters of the chemisorption interaction with the substrate. The constants k_{D1} and k_{D2} should be compared with each other (the nature of interaction with the adsorption centers is the same), as well as the value of the constants ratio for different substrates. For the group of tissue pectins, the relative index value is approximately the same (1.23–1.26). For P_{MIGR}, the constants ratio has increased to 2.04, which indicates simultaneously the absence of obstacles to maintaining the sorbate concentration gradient in the surface layer and the increased resistance to the intradiffusion processes.

The ratio of the constants k_{D1} and k_{D2} can change significantly during the transition to real processes taking place in the digestive tract of ruminants when the external environment is represented by a thick mass of the digested fodder mixture. Modeling of the mass transfer under approximate conditions will be the subject of further research. At the same time, it is obvious that external impurities do not change the state of the swollen grain of pectin sorbents and the dynamics of the internal mass transfer, the intensity of which is determined by the features of the chemical and supramolecular structure of the biopolymer.

The obtained values of the effective diffusion coefficient make it possible to quantitatively characterize the dependence of the mass transfer limiting stage in the volume of hydrated pectin particles on the features of the structural arrangement of polyuronides, illustrated in Fig. 4. The P_{BAST} preparation particles with an openwork mesh supramolecular structure possess the greatest permeability. A reduction in the cell size of mesh domains in the P_{PAR} preparation particles naturally manifests itself in a decrease in the coefficient D by 4.5 times.

The decrease of the theophylline diffusion coefficient D by an order of magnitude for the preparation P_{XYL} indicates that after the release from lignocellulose reinforcement, the ribbon formations of paired macromolecules are formed into bundles. The increased density of the bundle, apparently, causes the complete absence of zones of the water own structure and strong structuring of its molecules in the zones of near and far hydration of polymer chains, which complicates the movement of theophylline in the particle volume. In the cellular structure of P_{PAR} and especially P_{BAST}, free water is apparently present and its amount correlates with the cells size.

In this case, the decrease in the effective diffusion coefficient D for the P_{MIGR} preparation by 4 decimal orders relative to the P_{XYL} values can only be associated with the increase in the thickness and density of the near hydration zone of branches with a high content of unsubstituted monomer units and dissociating carboxyl groups. The manifestation of hydration of such sites has been considered when analyzing the influence of the medium acidity on the theophylline equilibrium sorption results. According to the diagram in Fig. 4c, the increased diffusion resistance zones are sections of flexible segments with the closest location of unsubstituted units, which are directly adjacent to the “egg-box” crosslink. The ultra-low value of the internal diffusion coefficient explains the sharp slowdown of sorption when the 75% saturation of the polymer is reached.

The positive point is that the internal diffusion does not control the initial stage of the sorption process, which provides the main contribution to the achievement of the highest sorption capacity level of the P_{MIGR} preparation in comparison with the application efficiency of flax tissue pectins.

Analysis of the kinetic models of theophylline sorption. The practical tasks to describe the stationary sorption process kinetics include the evaluation of constants, reflecting the dynamics changes as the system approaches equilibrium, as well as the determination of the calculated value of the capacity limit q_e* and the degree of approximation to it under experimental conditions. The Lagergren pseudo-first-order and the Ho and McKay pseudo-second-order kinetic models have been used to analyze the empirical data [61–63]. Both description options assume that the interaction of the sorbed substance with the adsorption centers limits the sorption process. In the first case, modeling covers a wide range of processes, in which diffusion precedes sorption. The second option correctly describes the chemical interaction processes between the sorbate and the functional groups of the sorbent.

The models applicability is determined by the possibility of linear approximation of the kinetic dependencies by correlation relations of the following type:

—pseudo-first-order model:

$$\ln(q_e - q_t) = \ln q_e^* - k_1 t;$$

—pseudo-second-order model:

$$t/q_t = 1/(k_2 q_e^{*2}) + t/q_e^*,$$

where k_1 is the pseudo-first-order adsorption rate constant, min^{-1}; k_2 is the pseudo-second-order adsorption rate constant, g mmol^{-1} min^{-1}.

It is accepted to demonstrate the empirical data description adequacy graphically in the coordinates of ln ($q_e - q_t$) from t for the Lagergren model and in the coordinates of t/q_t from t for the Ho and McKay model. In the first case, the k_1 constant value is calculated based on the approximating dependency angle and the calculated limit sorption value of the material q_e* is determined by extrapolation to the initial moment of the sorption process. In the second option, the values of q_e* are calculated

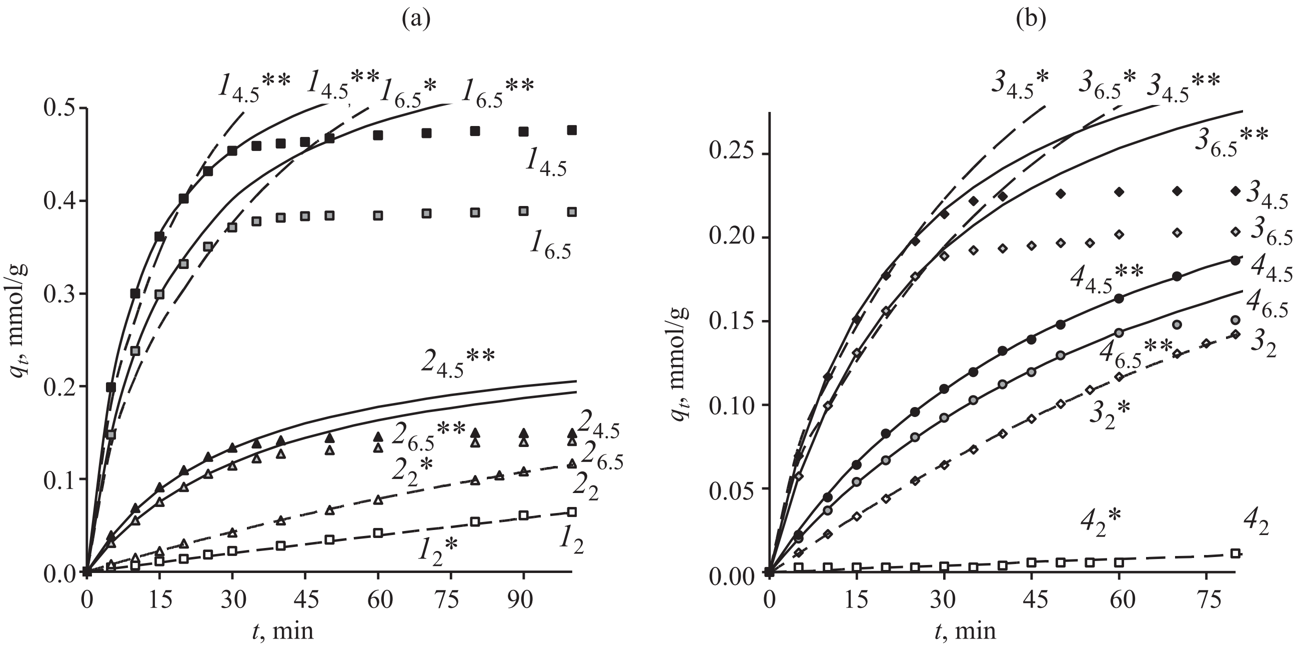

Fig. 9. Kinetics of theophylline sorption (points) by pectin preparations (a) P_{MIGR} and P_{PAR}, (b) P_{BAST} and P_{XYL} and approximating dependencies (lines) with application of kinetic models: (1_2, $1_{4.5}$, $1_{6.5}$) P_{MIGR} at pH of 2, 4.5, and 6.5, respectively; (2_2, $2_{4.5}$, $2_{6.5}$) P_{PAR}; (3_2, $3_{4.5}$, $3_{6.5}$) P_{BAST}; (4_2, $4_{4.5}$, $4_{6.5}$) P_{XYL}; (1_{pH}*–4_{pH}*) kinetic model dependencies; (1_{pH}**–4_{pH}**) pseudo-second order kinetic model dependencies.

by the tangent of the linear dependency angle and the parameter k_2 is determined based on the free term value.

For the systems under study, the linear graphical interpretation of the sorption dependencies kinetic section at the pH values of 4.5 and 6.5 is obtained in the coordinates of the pseudo-second-order model and for a strongly acidic medium with the pH of 2—in the coordinates of the pseudo-first-order model. The correctness of use of the relevant models is demonstrated in Fig. 9 on the example of the P_{MIGR} and P_{BAST} preparations, for which the process description results by the Lagergren model (dashed lines $1_{4.5}$*, $3_{4.5}$* and $1_{6.5}$*, $3_{6.5}$*, respectively, for the pH values of 4.5 and 6.5 units) and by the pseudo-second-order model (solid lines $1_{4.5}$**, $3_{4.5}$** and $1_{6.5}$**, $3_{6.5}$**) are presented simultaneously.

The presented results clearly demonstrate that the absorption of theophylline by pectin substrates is accurately reproduced by the solid lines for the pseudo-second-order model in all cases when the acidity level suggests the chemisorption mechanism of the sorbate binding at the polymer functional centers. The sorption processes involving non-ionized pectin preparations in a strongly acidic medium are better described within the framework of the Lagergren model (see the dashed lines).

From the set of the calculated kinetic characteristics of the sorption process, presented in Table 4, first of all, attention should be paid to the value of q_e*. For each substrate, regardless of the theophylline absorption conditions and the type of the correctly applied kinetic model (taking into account pH), the same limit sorption value is reproduced. Moreover, these values are very close to the characteristic of the substrates sorption potential $Q_{\max}$, used in the analysis in Fig. 6 and determined, taking into account the fractional content of *GH* units in the polymer.

As the availability of unsubstituted galacturonate units significantly depends on their joint structural distribution with methoxylated and calcium-pectate monomer units, it is logical to obtain the justified limit sorption values q_e*, based on the results of physicochemical studies, that are below the value of the theoretically possible sorption potential $Q_{\max}$. As a result of the correlation analysis of the relationship between the limit sorption capacity of pectin substrates and their chemical structure, the following multi-parameter ratio has been obtained:

$$q_e^* = 0.887 + 1.0889GH - 0.1222 - aGM,\ r = 0.9775.$$

Table 4. Kinetic parameters of theophylline sorption by pectin preparations

Pectin	Pseudo-second-order model				Pseudo-first-order model	
	pH 4.5		pH 6.5		pH 2.0	
	k_2, g mmol^{-1} min^{-1}	q_e*, mmol/g	k_2, g mmol^{-1} min^{-1}	q_e*, mmol/g	k_1, min^{-1}	q_e*, mmol/g
P_{XYL}	0.051	0.326	0.039	0.326	0.0004	0.325
P_{PAR}	0.125	0.266	0.098	0.264	0.0058	0.268
P_{BAST}	0.131	0.366	0.101	0.365	0.0064	0.367
P_{MIGR}	0.158	0.609	0.104	0.608	0.0011	0.612

The coefficient a is equal to 0.0417 or 0.03, respectively, for low-methoxylated pectins ($GM < 0.5$; P_{XYL} and P_{MIGR}) or high-methoxylated preparations ($GM > 0.5$; P_{BAST} and P_{PAR}).

The regression model can be used to predict the preventive effect of pectin-containing sorbents on alkaloids based on data on the ratio of galacturonate units in the unsubstituted, methoxylated, and calcium-pectate forms in polyuronides. The obtained values of the adsorption rate and the limit sorption capacity constants make it possible to determine the dosage of pectin-containing fodder supplements to prevent mycotoxicosis based on the calculation of the specific binding of alkaloids during the 30-min passage of the digested fodder mass in the ruminants' duodenum, based on the integral equation of the pseudo-second-order adsorption model:

$$q_{30} = \frac{30}{\left(\frac{1}{k_2 q_e^{*2}} + \frac{30}{q_e^*}\right)}.$$

It is important to note that the alkaloids sorption process does not end when the fodder mixture moves into the small intestine and can continue at a slightly decreased rate in the presence of bile-pancreatic juice with the pH of 6.8. For tissue pectins, the constant k_2 decreases equally (1.27–1.29 times). For the P_{MIGR} preparation, the drop is more significant – by 1.51 times; however, the value of the indicator continues to be the highest for the compared substrates.

As noted in the comment to the obtained values of the external diffusion constant k_{D1} (see Table 3), in real systems, the sorbate mobility can be hindered due to the increased viscosity of the medium. The sorption process parameters at the pH of 2, presented in Table 4, make it possible to suggest that when the P_{BAST} and P_{PAR} preparations are applied, this problem can be largely eliminated due to the binding of theophylline in the highly acidic medium of the ruminants' stomach by the physical adsorption mechanism (see Fig. 5b). The preliminary accumulation of the sorbate in the swollen pectin grain during the two-hour stay of the fodder in the stomach will ensure the accelerated course of chemisorption interactions during the transition of the fodder mass into the intestine.

Regularity of theophylline absorption by flax pectin and montmorillonite compositions. The effectiveness of the pectin substrates action has been compared with the results of theophylline sorption by montmorillonite (Mt), a type of aluminosilicate sorbents, widely applied for the prevention of mycotoxicosis in animals.

In a strongly acidic medium, Mt exhibit almost no sorption properties with respect to theophylline and, as shown in Fig. 10a, increasing its sorption activity as the acidity decreases. The comparison of results with the data in Fig. 6a demonstrates that at the pH of 4.5 (the main value for the binding of mycotoxins in the ruminants' digestive tract) Mt exceeds the value of q_{120} for the P_{PAR} preparation by only 11.5%. The P_{XYL} and P_{BAST} preparations are 10 and 30% more efficient, whereas P_{MIGR} exceeds the sorption properties of the reference sample almost thrice.

The comparison by the sorption rate constant value does not seem possible, since at the pH of 4.5, the processes involving pectin substrates and Mt are described by different kinetic models. For Mt, the best description adequacy is provided by the pseudo-first-order model, which is demonstrated by the exact compliance of the empirical data with the course of the calculated curves

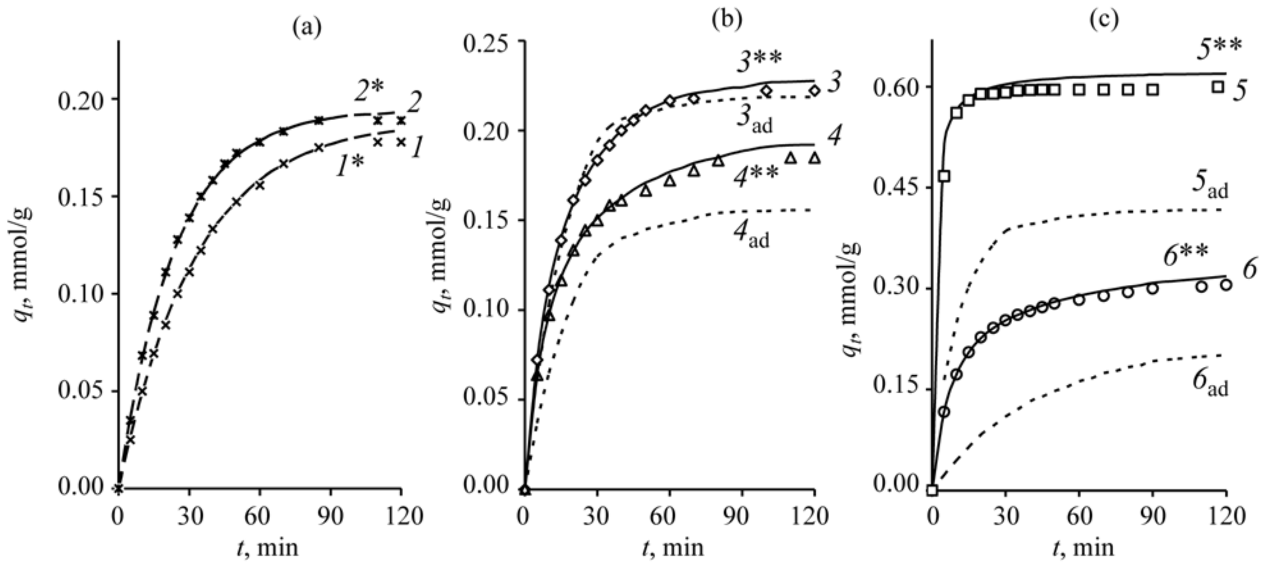

Fig. 10. Kinetics of theophylline sorption by montmorillonite (a) and binary montmorillonite preparations with pectins (b) and (c) in the ratio of 20 : 80: (*1*, *2*) empirical data (points) at pH of 4.5 and 6.5, respectively; (*1**, *2**) calculated dependencies according to the pseudo-first order model (dashed line); (*3*–*6*) empirical data for samples P_{BAST}–Mt, P_{PAR}–Mt, P_{MIGR}–Mt, and P_{PAR}–Mt at pH of 4.5; (*3***–*6***) calculated dependencies according to the pseudo-second order model (solid line); (3_{ad}–6_{ad}) calculated dependences of the components additive contribution (dotted line).

*1** and *2**. With an increase in the pH value from 4.5 to 6.5 units, the sorption rate constant k_1 increases from 0.0303 to 0.0418 min^{-1}. The visual comparison with the growth of the q_t index for polyuronides in Fig. 7a indicates that the Mt activity is comparable only with the least rapid sorption for the P_{XYL} preparation. The calculated limit sorption level for Mt is 0.1944 and 0.2028 mmol/g at the pH of 4.5 and 6.5, respectively, which is 1.3–3 times lower than the value of q_e* for pectin preparations.

Taking into account the increasing attention to the creation of hybrid polymer-inorganic sorbents based on aluminosilicates, modified with polyelectrolytes [90–93], the effectiveness of alkaloids binding with binary preparations of flax pectins and montmorillonite has been evaluated. The review [94] presents a critical analysis of the existing methods and mechanisms for exfoliation of layered aluminosilicates aimed to achieve the target effects of developing the inner surface of the mineral filler and giving specific functions to the created nanocomposites. The solid-phase method for production of organo-mineral systems, applied in work [56], suggests the surrounding of pectin microgranules with Mt particles, swollen in water, and makes it possible to regulate the degree of intercalation of the pectin polymer chains into the aluminosilicate interplanar spaces, depending on the degree of the macromolecules crosslinking by *GC* units.

According to the results of theophylline sorption studies, differences in the behavior of the model preparations, based on flax pectins, have been revealed. In case of the P_{BAST}–Mt sample (Fig. 10b), the calculated curve of the additive contribution (curve 3_{ad}) of the components, present in the preparation with a percentage ratio of 80 : 20, almost coincides with the dynamics of the empirical results growth (points *3*). Consequently, pectin particles do not possess the ability to penetrate into the interlayer spaces of Mt. The binary preparation components are present in the system and exhibit their sorption properties independently of each other. Moreover, the cumulative effect of the mixture is slightly inferior to the sorption capacity of P_{BAST} when applied individually.

In contrast, the sorption results for the P_{PAR}–Mt sample (points *4*) are significantly ahead of the curve of additive manifestation of the components activity (curve 4_{ad}). The reason for these differences should be sought in the features of the pectin preparations structure, illustrated in Fig. 4. Apparently, the indifference of P_{BAST} to the presence of Mt is less related to the larger cell size of mesh domains. A more important circumstance is the integral and undamaged character of the mesh structure in the volume of P_{BAST} particles, unlike the pectin of the stem parenchymal tissues, subjected to microbiological destruction in the flax dew retting processes. Figure 4b demonstrates the presence of end segments, which can penetrate into the interlayer spaces of the layered silicate, providing its exfoliation, in the P_{PAR} structure. The small sizes of the end branches limits the depth of intercalation, thereby preventing significant blocking of the Mt inner surface.

Contrary to fears, the P_{XYL}–Mt binary system components have also demonstrated their ability to interact under the composition production conditions. Moreover, the ribbon formations of the paired P_{XYL} macromolecules provide more effective exfoliation of Mt compared to the influence of the few and, what is important, thinner end branches in the structure of P_{PAR}. For the P_{XYL}–Mt composite, the superadditivity relative manifestation maximum has been recorded: the achieved equilibrium sorption value is 1.5 times higher than the additive index (curve 6_{ad}). It is especially important that the increment of the 30-min sorption (q_{30}) over the additive value reaches 2.3 times, while for the P_{MIGR}–Mt and P_{PAR}–Mt preparations the difference is 1.53 and 1.39 times.

In absolute terms, the maximum superadditivity effect is demonstrated by the P_{MIGR}–Mt system. It is not the only important point that the equilibrium sorption increment (points *5*) over the additive index (curve 5_{ad}) exceeds, for example, the calculated sorption capacity value for the P_{PAR}–Mt components according to curve 4_{ad}. The record large differences in the initial sections of the dependencies *5* and 5_{ad} are indicative: the increment of q_{10} is 0.311 mmol/g, which is half of the equilibrium value. The synergy in the development of the P_{MIGR}–Mt preparation sorption capacity is, apparently, provided by both components.

The electrostatic repulsion of branches with the opposite direction of dissociated carboxyl groups, illustrated in Fig. 4c, in the process of intercalation of the P_{MIGR} particles into the Mt structure, ensures the maximum increase in the interplanar distance of the layered aluminosilicate. At the same time, the space between the Mt layers is a kind of concentrator, increasing the sorbate content in the external environment for the pectin component, which intensifies chemisorption binding of theophylline at the P_{MIGR} adsorption centers.

Table 5. Kinetic parameters of theophylline sorption by pectin-montmorillonite preparations at pH of 4.5

Sorbent	k_2, g mmol^{-1} min^{-1}	k_2 (composite)/ k_2 (pectin)	q_e*, mmol/g
P_{XYL}–Mt	0.340	6.7	0.328
P_{PAR}–Mt	0.422	3.4	0.272
P_{BAST}–Mt	0.272	2.1	0.339
P_{MIGR}–Mt	1.494	9.5	0.625

The kinetics of theophylline sorption by binary preparations is adequately described within the framework of the Ho and McKay model, as evidenced by the course of the calculated dependencies *3***–*6***. The kinetic characteristics of the processes are compared in Table 5.

For convenience of comparison, the k_2 constant values are presented not only for the studied binary compositions, but also in relative terms to the value for the base pectin preparation (see Table 4). As can be seen, the former outsider (P_{XYL}) has significantly increased the adsorption rate and in terms of k_2 outperforms the vice-leader (P_{BAST}) in the ranking of pectin substrates. It is noteworthy that the presence of Mt still affects the properties of the P_{BAST} preparation, its effect manifested in the twofold increase in the constant k_2. Obviously, the adhesion of the Mt particles on the P_{BAST} grain surface provides the effect, noted for the P_{MIGR}–Mt system, increasing the theophylline concentration gradient in the surface layer, which contributes to the acceleration of chemisorption interactions in the grain structure.

The growth of the constant k_2 for the P_{MIGR}-based composite is indicative; although it is not accompanied by a noticeable increase in the limit sorption for P_{MIGR}–Mt. In this system, the sorption potential realization degree is almost 100% implemented and in case of individual application of Mt, exceeds the value of q_e* by 3.2 times. The obtained results substantiate the expediency to use the water-soluble fraction of polyuronides in flax shive to create specialized hybrid means for the prevention of mycotoxicosis in animals and humans. The parameters of k_2 and q_e* for P_{MIGR}–Mt make it possible to determine the daily consumption dosage of the highly effective composite sorbent, using the equation of the pseudo-second-order adsorption kinetic model.

Thus, the identified patterns of the influence of the chemical structure of pectin substances on their sorption properties with respect to theophylline make it possible to regulate the type of flax processing by-products, applied to obtain flax-containing fodder supplements, to evaluate the effectiveness of their use for the binding of azaheterocyclic mycotoxins, and to scientifically substantiate the sorbents consumption rate standards for the prevention of mycotoxicosis in ruminants.

CONCLUSIONS

1. The difference of pectin substances, contained in the parenchyma, bast, and wood tissues of flax processing by-products, has been evaluated by the IR spectroscopy and viscometry methods. According to the data on the fractional ratio of galacturonate units with the unsubstituted carboxyl group, as well as in the methoxylated and calcium-pectate forms, modeling of the supramolecular structure of the obtained tissue pectin preparations, as well as the water-soluble fraction of polyuronides, extracted from flax shive, has been performed.

2. The absorption of theophylline by pectin preparations from diluted aqueous solutions at a temperature of 40°C and a variable pH value of 2.0, 3.5, 4.5, and 6.5 has been investigated by the method of stationary sorption from the limited volume. The correlations between the values of the equilibrium sorption of theophylline and the parameters of the pectin grain supramolecular structure have been identified.

3. The analysis of sorption curves, using the Boyd and Weber-Morris diffusion models, has revealed a mixed diffusion mode of the mass transfer at the pH of 4.5, has made it possible to determine the duration of the initial sorption stage, complicated by external diffusion, and to compare the diffusion rate constant values for the external and internal diffusion limitation stages. With the application of the gel diffusion model, it has been possible to determine the values of the effective diffusion coefficient for theophylline in the volume of hydrated pectin particles, the change in which is consistent with the ideas about the formation of the supramolecular structure of polyuronides and the specifics of the hydration environment of different forms of galacturonate units.

4. The application of the Lagergren kinetic models to describe the sorption of theophylline at the pH of 2.0 and the Ho and McKay kinetic model for the sorption process in solutions with the pH values of 4.5 and 6.5 has been justified. The values of the limit sorption index q_e* for the compared polyuronide substrates have been determined and a correlation model has been developed to predict the limit sorption capacity of pectin sorbents with respect to alkaloids, based on the data on the fractional ratio of the forms of galacturonate units. The practical value of the obtained data on the adsorption rate constant k_2 and the index q_e* is associated with the possibility to justify the dosage of fodder supplements, containing different types of pectin-containing flax materials to prevent mycotoxicosis of ruminants, provoked by numerous types of azaheterocyclic mycotoxins.

5. The superiority of pectin preparations as compared with montmorillonite, a variety of widely used alumino-silicate sorbents, has been demonstrated. The sorption of theophylline by binary pectin-montmorillonite preparations in the ratio of 80 : 20 has been investigated. The differences in the demonstrated effects of the superadditive sorption capacity of the composites are associated with the features of the pectins supramolecular structure and the possibilities of regulated intercalation of polymer chains in the layered mineral structure.

FUNDING

The research works are carried out within the framework of the State Assignment of the G.A. Krestov Institute of Solution Chemistry of the Russian Academy of Sciences (project no. 01201260483) using the instrument base of the Centre for joint use of scientific equipment "The upper volga region center of physico-chemical research."

CONFLICT OF INTEREST

No conflict of interest was declared by the authors.

REFERENCES

1. Khorshidi, S., Karkhaneh, A., Bonakdar, S., and Omidian, M.M., *J. Appl. Polym. Sci.*, 2019, vol. 137, no. 28, p. 48859. https://doi.org/10.1002/app.48859
2. Ghorbani, M., Roshangar, L., and Rad, J.S., *Eur. Polym. J.*, 2020, vol. 130, p. 109697. https://doi.org/10.1016/j.eurpolymj.2020.109697
3. Sathya, U., Nithya, M., and Keerthi, P., *Chem. Phys. Lett.*, 2020, vol. 744, p. 137201. https://doi.org/10.1016/j.cplett.2020.137201
4. Yunlong, J. and Bodo, F., *Composites Commun.*, 2020, vol. 18, pp. 5–12. https://doi.org/10.1016/j.coco.2019.12.010
5. Chabbert, B., Padovani, J., Djemiel, C., Ossemond, J., Lemaitre, A., Yoshinaga, A., Hawkins, S., Grec, S., Beaugrand, J., and Kurek, B., *Industrial Crops and Products*, 2020, vol. 148, p. 112255. https://doi.org/10.1016/j.indcrop.2020.112255

6. Niwinska, B., *Digestion in Ruminants, Carbohydrates – Comprehensive Studies on Glycobiology and Glycotechnolo*, Chang, Ch.-F., Ed., CC BY, 2012, pp. 245–258. https://doi.org/10.5772/51574
7. Beigh, Y.A., Ganai, A.M., and Ahmad, H.A., *Vet. World*, 2017, vol. 10, no. 4, pp. 424–437. https://doi.org/10.14202/vetworld.2017.424-437
8. Kelzer, J.M., Kononoff, P.J., Tedeschi, L.O., Jenkins, T.C., Karges, K., and Gibson, M.L., *J. Dairy Sci*., 2010, vol. 93, pp. 2803–2815. https://doi.org/10.3168/jds.2009-2460
9. Yildiz, E. and Todorov, N., *Bulgarian J. Agric. Sci*., 2014, vol. 20, pp. 428–446.
10. Marghazani, I.B., Jabbar, M.A., Pasha, T.N., and Abdullah, M., *Ital. J. Anim. Sci.*, 2012, vol. 11, no. 1, pp. 58–62. https://doi.org/10.4081/ijas.2012.e11
11. Jayanegaraa, A., Dewib, S.P., and Ridlaa, M., *Media Peternakan*., 2016, vol. 39, no. 3, pp. 195–202. https://doi.org/10.5398/medpet.2016.39.3.195
12. Adiwinarti, R., Kustantinah, K., Budisatria, I.G.S., Rusman, R., and Indarto, E., *Asian J. Anim. Sci*., 2016, vol. 10, no. 4, pp. 262–267. https://doi.org/10.3923/ajas.2016.262.267
13. Goh, C.H., Nicotra, A.B., and Mathesius, U., *Plant Cell Environ*., 2016, vol. 39, pp. 883–896. https://doi.org/10.1111/pce.12672
14. Laconi, E.B. and Jayanegara, A., *Asian Australas. J. Anim. Sci*., 2015, vol. 28, pp. 343–350. https://doi.org/10.5713/ajas.13.0798
15. Mahima, Kumar, V., Tomar, S.K., Roy, D., and Kumar, M., *Vet. World*, 2015, vol. 8, pp. 551–555. https://doi.org/10.14202/vetworld.2015.551-555
16. Adiwinarti, R., Budisatria, I.G.S., Kustantinah, K., Rusman, R., and Indarto, E., *Vet. World*, 2019, vol. 12, pp. 890–895 https://doi.org/10.14202/vetworld.2019.890-895
17. Csapo, J., Albert, Cs., and Kiss, D., *Acta Univ. Sapientiae, Alimentaria*, 2018, vol. 11, pp. 110–127. https://doi.org/10.2478/ausal-2018-0007
18. Ayyat, M.S., Al-Sagheer, A., Noreldin, A.E., Abdel-Hack, M.E., Khafaga, A.F., Abdel-Latif, M.A., Swelum, A.A., Arif, M., and Salem, A.Z.M., *Anim. Biotechnol.*, 2019, pp. 1–16. https://doi.org/10.1080/10495398.2019.1653314
19. Kamalak, A., Canbolat, O., Gurbuz, Y., and Ozay, O., *KSU J. Sci. Eng.*, 2005, vol. 8, no. 2, p. 84–88.
20. Grudina, N.V., Grudin, N.S., and Bydanova, V.V., *Dokl. Ros. Akad. Sel'khoz. Nauk*, 2015, no. 6, pp. 47–49.
21. Peixoto, E.L.T., Morenz, M.J.F., Da Fonseca, C.E.M., Dos Santos Moura, E., De Lima, K.R., Lopes, F.C.F., and Da Silva Cabral, L., *Semin. Agrar*., 2015, vol. 36, pp. 3421–3430. https://doi.org/10.5433/1679-0359.2015v36n5p3421
22. Foiklang, S., Wanapa, M., and Norrapoke, T., *Asian-Australas. J. Anim. Sci.*, 2016, vol. 29, pp. 1416–1423. https://doi.org/10.5713/ajas.15.0689
23. Tayengwa, T. and Mapiye, C., *Sustainability*, 2018, vol. 10, no. 10, p. 3718. https://doi.org/10.3390/su10103718
24. Zhao, G., Diao, H.-J., and Zong, W., *Food Sci. Technol. Int.*, 2013, vol. 19, no. 2, p. 153. https://doi.org/10.1177/1082013212442191
25. Aleeva, S.V., Lepilova, O.V., and Koksharov, S.A., *Izv. Vuzov: Tekhnol. Tekstil. Prom–ti*, 2017, no. 1, pp. 319–324.
26. Aleeva, S.V., Lepilova, O.V., Kurzanova, P.Yu., and Koksharov, S.A., *Izv. Vuzov: Khim. Khim. Tekhnol.*, 2018, vol. 61, no. 2, pp. 80–85. https://doi.org/10.6060/tcct.20186102.5512
27. Aleeva, S.V., Lepilova, O.V., and Koksharov, S.A., *Izv. Vuzov: Tekhnol. Tekstil. Prom–ti*, 2018, no. 4, pp. 89–95.
28. Koksharov, S.A., Aleeva, S.V, and Lepilova, O.V., *Int. J. Chem. Eng.*, 2019, 4137593, pp. 1–11. https://doi.org/10.1155/2019/4137593
29. RU Patent 2666769, 2018; *Byul. Izobret*., 2018, no. 26.
30. Dawod, A., Ahmed, H., Abou-Elkhair, R., Elbaz, H.T., Taha, A.E., Swelum, A.A., Alhidary, I.A., Saadeldin, I.M., Al-Ghadi, M.Q., Ba-Awadh, H.A., Hussein, E.O.S, and Al-Sagheer, A.A., *Animals*, 2020, vol. 10, no. 3, p. 436. https://doi.org/10.3390/ani10030436
31. Broderick, G. and Muck, R.E., *J. Dairy Sci.*, 2009, vol. 92, no. 3, pp. 1281–1303. https://doi.org/10.3168/jds.2008-1303
32. Rouches, E., Herpoel-Gimbert, I., Steyer, J.P., and Carrere, H., *Sustainable Energy Rev*., 2016, vol. 59, pp. 179–198. https://doi.org/10.1016/j.rser.2015.12.317
33. Bennett, J.W. and Klich, M., *Clin. Microbiol. Rev*., 2003, vol. 16, no. 3, pp. 497–516. https://doi.org/10.1128/CMR.16.3.497-516.2003
34. Akhmadyshin, R.A., Kanarskii, A.V., and Kanarskaya, Z.A., *Vest. Kazan. Tekhnolog. Univ.*, 2007, no. 2, pp. 88–103.
35. Gruber-Dorninger, C., Novak, B., Nagl, V., and Berthiller, F., *J. Agricult. Food Chem.*, 2017, vol. 65, no. 33, pp. 7052–7070. https://doi.org/10.1021/acs.jafc.6b03413

36. Wielogórska, E., MacDonald, S., and Elliot, C.T., *World Mycotoxin*, 2016, vol. 9, pp. 419–433. https://doi.org/10.3920/WMJ2015.1919
37. Vila-Donat, P., Marn, S., Sanchis, V., and Ramos, A.J., *Food. Chem. Toxicol.*, 2018, vol. 114, pp. 246–259. https://doi.org/10.1016/j.fct.2018.02.044
38. Freimund, S., Sauter, M., and Rys, P., *J. Environ. Sci. Health*, 2003, vol. 38, pp. 243–255. https://doi.org/10.1081/PFC-120019892
39. Yiannikouris, A., Francoi, J., Poughon, L., Dussap, C.G., Bertin, G., Jeminet, G., and Jouany, J.P., *J. Agricult. Food Chem.*, 2004, vol. 52, pp. 3666–3673. https://doi.org/10.1021/jf035127x
40. Nordi, E.C.P., Costa, R.L.D., David, C.M.G., Parren, G.A.E., Freitas, A.C.B., Lameirinha, L.P., Katiki, L.M., Bueno, M.S., Quirino, C.R., Gama, P.E., Bizzo, H.R., and Chagas, A.C.S., *Vet. Parasitol*., 2014, vol. 205, pp. 532–539. https://doi.org/10.1016/j.vetpar.2014.09.015
41. *Maksimal'no dopustimye urovni (MDU) mikotoksinov v kormakh dlya sel'skokhozyaistvennykh zhivotnykh* (Maximum Permissible Levels (MPL) of Mycotoxins in Farm Animals Fodder, no. 434-7, 01.02.89.
42. Rodrigues, I. and Naehrer, K., *Toxins*, 2012, vol. 4, pp. 663–675. https://doi.org/10.3390/toxins4090663
43. Pinto, V.E. and Patriarca, A., *Methods Mol Biol*., 2017, vol. 1542, pp. 13–32. https://doi.org/10.1007/978-1-4939-6707-0_2
44. Kozak, L., Szilagyi, Z., Toth, L., Pocsi, I., and Molnar, I., *Appl. Microbiol Biotechnol*., 2019, vol. 103, no. 4, pp. 1599–1616. https://doi.org/10.1007/s00253-018-09594-x
45. Manafi, M., Narayanaswamy, H.D., and Pirany, N., *African J. Agricult. Res.*, 2009, vol. 4, pp. 141–143. https://doi.org/10.3390/toxins10120510
46. Kudryashov, A.Yu., Koksharov, S.A., and Pashin, E.L., *Izv. Vuzov: Tekhnol. Tekstil. Prom–ti*, 2009, no. 5, pp. 3–5.
47. Koksharov, S.A., Aleeva, S.V., Skobeleva, O.A., and Kudryashov, A.Yu., *Izv. Vuzov: Khim. Khim. Tekhnol.*, 2011, vol. 54, no. 6, pp. 93–96.
48. Aleeva, S.V. and Koksharov, S.A., *Russ. J. Gen. Chem*., 2012, vol. 82, no. 13, pp. 2279-2293. https://doi.org/10.1134/S1070363212130154
49. Koksharov, S., Aleeva, S., and Lepilova, O., *Autex Res. J*., 2015, vol. 15, no. 3, pp. 215–225. https://doi.org/10.1515/aut-2015-0003
50. Aleeva, S.V., Chistyakova, G.V., Lepilova, O.V., and Koksharov, S.A., *Russ. J. Phys. Chem. A*, 2018, vol. 92, no. 8, pp. 1583–1589. https://doi.org/10.1134/S0036024418080022
51. Koksharov, S.A., Aleeva, S.V., and Lepilova, O.V., *Mol. Liq.*, 2019, vol. 283, pp. 606–616. https://doi.org/10.1016/j.molliq.2019.03.109
52. Lepilova, O.V., Koksharov, S.A., and Aleeva, S.V., *Russ. J. Appl. Chem.*, 2018, vol. 91, no. 1, pp. 90–95. https://doi.org/10.1134/S1070427218010147
53. Koksharov, S.A., Aleeva, S.V, and Lepilova, O.V., *Key Eng. Mater.*, 2019, vol. 816, pp. 333–338. https://doi.org/10.4028/www.scientific.net/KEM.816.333
54. Koksharov, S.A. and Aleeva, S.V., *Scientific Foundations of the Carbohydrates Chemical Technology*, Zakharov, A.G., Ed., Moscow: Izd. LKI, 2008, pp. 401–523.
55. Ivanchenko, O., Aronova, E., Balanov, P., and Smotraeva, I., *IOP Conf. Series: Earth and Environmental Science*, 2019, vol. 337, 012037. https://doi.org/10.1088/1755-1315/337/1/012037
56. Kochkina, N.E., Skobeleva, O.A., and Khokhlova, Yu.V., *Particul. Sci. Technol*., 2017, vol. 35, no. 3, pp. 259–264. https://doi.org/10.1080/02726351.2016.1153546
57. Aleeva, S.V., Chistyakova, G.V., and Koksharov, S.A., *Izv. Vuzov: Khim. Khim. Tekhnol.*, 2009, vol. 52, no. 10, pp. 118–121.
58. Boyd, G.E., Adamson, A.W., and Myers, L.S., *J. Am. Chem. Soc*., 1947, vol. 69, pp. 2836–2848.
59. Weber, Jr.W.J. and Morris, J.C., *J. Sanit. Eng. Div*., 1963, vol. 89, pp. 31–59.
60. Maslova, M.V., Ivanenko, V.I., and Gerasimova, L.G., *Russ. J. Phys. Chem. A*, 2019, vol. 93, no. 7, pp. 1245–1251. https://doi.org/10.1134/S0036024419060219
61. Ho, Yu.Sh., Ng, J.C.Y., and McKay, G., *Separat. Purificat. Methods*, 2000, vol. 2, no. 29, pp. 189–232. https://doi.org/10.1081/SPM-100100009
62. Ho, Yu.Sh., *Scientometrics*, 2004, vol. 1, no. 59, pp. 171–177. https://doi.org/10.1023/B:SCIE.0000013305.99473.cf
63. Douven, S., Paez, C.A., and Gommes, C.J., *J. Colloid Interface Sc.*, 2015, vol. 448, pp. 437–450. https://doi.org/10.1016/j.jcis. 2015.02.053
64. Shepherd, W., *Materiae Vegetabiles*, 1956, vol. 2, pp. 58–63. https://doi.org/10.1007/BF01889775
65. Pretsch, E., Buhlmann, Ph., Badertscher, M., *Structure Determination of Organic Compounds: Tables of Spectral

Data, Berlin: Springer-Verlag Berlin Heidelberg, 2009, pp. 269–336.
66. Khotimchenko, M., Kovalev, V., and Khotimchenko, Yu., *J. Hazardous Mater*., 2007, vol. 149, pp. 693–699. https://doi.org/10.1016/j.jhazmat.2007.04.030
67. Kaisheva, N.Sh. and Kaishev, A.Sh., *Russ. J. Phys. Chem A*, 2015, vol. 89, no. 7, p. 1216. https://doi.org/10.7868/S0044453715070146
68. Yapo, B.M. and Koffi, K.L., *Carbohydr. Polym*., 2013, vol. 92, no. 1, pp. 1–10 https://doi.org/10.1016/j.carbpol.2012.09.010
69. Zhang, B., Hu, B., Nakauma, M., Funami, T., Nishinari, K., Draget, K.I., Phillips, G.O., and Fang, Y., *Food Res. Int*., 2019, vol. 116, pp. 232–240 https://doi.org/10.1016/j. foodres.2018.08.020
70. Morris, E.R., Powell, D.A., Gidley, M.J., and Rees, D.A., *J. Mol. Biol.*, 1982, vol. 155, no. 4, pp. 517–531. https://doi.org/10.1016/0022-2836(82)90484-3
71. Padayachee, A., Day, L., Howell, K., and Gidley, M.J., *Critical Rev. Food Sci. Nutrit.*, 2017, vol. 57, no. 1, pp. 59–81. https://doi.org/10.1080/10408398.2013.850652
72. Assifaoui, A., Lerbret, A., Uyen, H.T.D., Neiers, F., Chambin, O., Loupiac, C., and Cousinc, F., *Soft Matter*, 2015, vol. 11, no. 3, pp. 551–560. https://doi.org/10.1039/c4sm01839g.
73. Plazinski, W., *J. Comput. Chem*., 2011, vol. 32, no. 14, pp. 2988–2995 https://doi.org/10.1002/jcc. 21880
74. Gawkowska, D., Cybulska, J., and Zdunek, A., *Polymers*, 2018, vol. 10, pp. 762–787. https://doi.org/10.3390/polym10070762
75. Mikshina, P.V., Petrova, A.A., Faizullin, D.A., Zuev, Yu.F., and Gorshkova, T.A., *Biochemistry (Moscow)*, 2015, vol. 80, no. 7, pp. 915–924. https://doi.org/10.1134/S000629791507010X
76. Day, A., Ruel, K., Neutelings, G., Cronier, D., David, H., Hawkins, S., and Chabbert, B., *Planta*, 2005, vol. 222, pp. 234–245. https://doi.org/10.1007/s00425-005-1537-1
77. Huis, R., Morreel, K., Fliniaux, O., Lucau-Danila, A., Fénart, S., Grec, S., Neutelings, G., Chabbert, B., Mesnard, F., Boerjan, W., and Hawkins, S., *Plant Physiol.*, 2012, vol. 158, no. 4, pp. 1893–1915 https://doi.org/10.1104/PP. 111. 192328
78. Khotimchenko, M., Makarova, K., Khozhaenko, E., and Kovalev, V., *Int. J. Biol. Macromol*., 2017, vol. 97, pp. 526–535. https://doi.org/10.1016/j. ijbiomac.2017.01.065
79. Chistyakova, G.V. and Koksharov, S.A., *Russ. J. Gen. Chem*., 2014, vol. 84, no. 4, pp. 763–766. https://doi.org/10.1134/S1070363214040276
80. Jakóbik-Kolon, A., Mitko, K., and Bok-Badura, J., *Materials*, 2017, vol. 10, no. 7, pp. 844–855 https://doi.org/10.3390/ma10070844
81. Boumediene, M., Benaïssa, H., George, B., Molina, St., and Merlin, A., *J. Mater. Environ. Sci*., 2018, vol. 9, no. 6, pp. 1700–1711. https://doi.org/10.26872/jmes.2018.9.6.190
82. Hurairah, S.N., Lajis, N.M., and Halim, A.A., *J. Geosci. Environ. Protect.*, 2020, vol. 8, no. 2, pp. 128–143. https://doi.org/10.4236/gep.2020.82009
83. Kumar, N.S., Asif, M., Poulose, A.M., Suguna, M., and Al-Hazza, M.I., *Processes*, 2019, vol. 7, no. 10, p. 757. https://doi.org/10.3390/pr7100757
84. Chatterjee, A. and Schiewer, S., *Chem. Eng. J.*, 2014, vol. 224, pp. 105–116. https://doi.org/10.1016/j. cej.2013.12.017
85. Korzh, E.A., Smolin, S.K., and Klymenko, N.A., *J. Water Chem. Technol.*, 2016, vol. 38, no. 4, pp. 187–193. https://doi.org/10.3103/S1063455X16040019
86. Campos, N.F., Barbosa, C.MBM, Rodrıguez-Dıaz, J.M., and Duarte, M.M.M.B., *Adsorpt. Sci. Technol.*, 2018, vol. 36, no. 1, pp. 1–17. https://doi.org/10.1177/0263617418773844
87. Ma, Y., Zhang, B., Ma, H, Yu, M., Li, L., and Li, J., *Sci. China Mater*., 2016, vol. 59, no. 1, pp. 38–50. https://doi.org/10.1007/s40843-016-0117-y
88. Sazonova, V.F., Perlova, O.V., Perlova, N.A., and Polikarpov, A.P., *Colloid. J*., 2017, vol. 79, no. 2, pp. 270–277. https://doi.org/10.1134/S1061933X17020132
89. Polyanskii, N.G., Gorbunov, G.V., and Polyanskaya, N.L., *Metody issledovaniya ionitov* (Methods for Ion Exchangers Studies), Moscow: Khimiya, 1976.
90. Varadwaj, G.B.B., Parida, K., and Nyamori, V.O., *Inorg. Chem. Front*., 2016, vol. 3, pp. 1100–1111. https://doi.org/10.1039/C6QI00179C
91. Wang, R.H., Zhu, X., Qian, W., and Hong, Z., *J. Soils Sediment.*, 2017, vol. 17, no. 10, pp. 1–9. https://doi.org/10.1007/s11368-017-1702-8
92. Tuchowska, M., Muir, B., Kowalik, M., Socha, R.P., and Bajda, T., *Materials*, 2019, vol. 12, p. 2253. https://doi.org/10.3390/ma12142253
93. Kon’kova, T.V., Morozov, A.N., Kandelaki, G.I., and Alekhina, M.B., *Russ. J. Phys. Chem. A*, 2018, vol. 92, no. 11, pp. 2135–2138. https://doi.org/10.1134/S0036024418110171
94. Zhu, T.T., Zhou, C.H., Kabwe, F.B., and Wu, Q.Q., *Appl. Clay Sci.*, 2019, vol. 169, pp. 48–66. https://doi.org/10.1016/j. clay.2018.12.006